Measurements of Methane Pyrolysis in a Constant Volume Batch Reactor at High Temperatures and Pressures

by

James Tatum

A thesis submitted in partial fulfillment of the requirements for the degree of

Master of Science

Department of Mechanical Engineering
University of Alberta

© James Tatum, 2021

Abstract

Methane pyrolysis is a process used to generate hydrogen gas and carbon black without the creation of carbon dioxide. Methane pyrolysis in a constant volume batch reactor was investigated at temperatures of 892 K, 1093 K, and 1292 K with reaction times of 15 s, 30 s, 60 s, 180 s, and 300 s with an initial pressure of 399 kPa. A quartz vessel (32 ml) was placed inside an oven where it was heated to high temperatures. The temperature and pressure inside the vessel were measured during the reaction. To begin the process, the quartz vessel was vacuumed, then flushed with nitrogen before being vacuumed again prior to every experiment. Pressurized methane was then injected into the vessel for an allocated reaction time and collected in a sample bag post reaction for analysis. The molar concentration of the product gas was analyzed using gas chromatography. Due to the accumulation of carbon on the vessel after a reaction, the vessel was cleaned with high pressure air after each experiment.

Hydrogen molar concentration increased as temperature and reaction time increased. For experiments completed at 892 K the hydrogen molar concentration varied from 10.0 ± 5.9 % with a 15 s reaction time to 26.5 ± 0.8 % for a 300 s reaction time. For experiments completed at 1093 K the hydrogen molar concentration varied from 21.8 ± 3.7 % for a 15 s reaction time to 53.0 ± 2.9 % for a 300 s reaction time. For experiments completed at 1292 K the hydrogen molar concentration varied from 31.5 ± 1.7 % for a 15 s reaction time to 53.0 ± 2.4 % for a 300 s reaction time.

Minor species concentrations were the greatest for experiments completed at 1292 K when compared to 892 K and 1093 K. There was a general decrease in minor species concentration for experiments completed at 1093 K when compared to 892 K. The summation of all minor species molar concentrations never exceeded 1 % of the total species detected.

Preface

This thesis is original work by James Tatum. Part of Chapter 1 and 2 of this thesis have been published as J. Tatum, A. Punia, M. Secanell, L. Kostiuk, and J. Olfert*. “Analysis of the products and kinetic rates of methane thermal decomposition. Part I: Experimental Apparatus”. In *Proceedings of Combustion Institute – Canadian Section, Spring Technical Meeting,* Kelowna, Canada May 13 – 16, 2019.

*Corresponding author: jolfert@ualberta.ca

Acknowledgements

I would like to sincerely thank Dr. Jason Olfert who supported and guided me throughout my research and for always believing in my work. I would not have been able to finish without his positive attitude and reinforcement. I would also like to thank Dr. Marc Secanell for his continued support throughout my entire project. Also, thanks to Dr. Larry Kostiuk for supporting this project and helping me get started. I am also grateful for Ambuj Punia for being my research partner and always helping me when I needed it. I am thankful that they all stuck with me and supported me through my spinal surgery.

Special thanks to my family, especially my parents for their unconditional love and support. Also, thanks to my stepmom, Dr. Evelyn Steinhauer, who always motivated me to strive to do more throughout my schooling. Thanks to my friends for helping me whenever I needed it.

Finally, I would like to thank Farjad Falahati and my other lab mates for helping me setup my experiments and for teaching me all the lab skills I needed to complete this research.

Table of Contents

List of Tables

List of Figures

1 Introduction

1.1 Motivation

Methane pyrolysis is the dissociation of methane into carbon black and hydrogen gas and is given as (Abbas and Wan Daud 2010):

$$\mathrm{CH_4} \rightarrow 2\mathrm{H_2} + \mathrm{C_{(s)}}, \qquad h_\mathrm{f}^\circ = -74.85\ \mathrm{kJ/kmol} \tag{1.1}$$

where, h_f° is the enthalpy of formation of CH_4. In practice other hydrocarbons are generated such as ethane and ethylene as well as aromatic hydrocarbons such as benzene. This reaction depends on temperature and reaction time and does not have high conversion into hydrogen until temperatures of > 1273 K without the use of a catalyst (Riley *et al.* 2021). However, with a catalyst this reaction could have high conversion into hydrogen at temperatures less than 973 K (Riley *et al.* 2021). Either way the products of methane pyrolysis are at high temperatures and the hydrogen and carbon black can be utilized in many applications

Methane pyrolysis has the advantage of being a way to generate energy from a fossil fuel without the creation of carbon dioxide. Methane pyrolysis has the potential to help combat global warming when renewable energy is not sufficient for high energy demand (Sánchez-Bastardo *et al.* 2020). Greenhouse-gas (GHG) emissions are increasing annually which has a major influence on the environment such as decreasing the pH of the ocean and increasing the atmospheric temperature (Abbas and Wan Daud 2010). This is because the use of fossil fuels for transportation, heating and power is still on the rise which results in the release of carbon dioxide into the atmosphere. Fossil fuels currently hold the largest market share for energy consumption at 87 % whereas renewable energy only accounts for 2 % (Ashik *et al.* 2015). Carbon dioxide emissions

are the main source of GHG making up 76 % (38 ± 3.8 $GtCO_2eq/yr.$ of the total 49 ± 4.5 $GtCO_2eq/yr.$) of all GHG emission in 2010 with 65 % (32 ± 2.7 $GtCO_2eq/yr.$ of the total 49 ± 4.5 $GtCO_2eq/yr.$) coming from fossil fuels and industrial processes (IPCC 2014). Human activities that generate GHG emissions are already estimated to have increased global warming by 1.0 ˚C when compared to preindustrial levels (Allen *et al.* 2018). If no action is taken to combat the carbon dioxide emissions global warming could increase to 2.0 ˚C by 2060 (IPCC 2014). By acting and reducing carbon dioxide emissions global warming could be limited to 1.5 ˚C (IPCC 2014). An alternate way of creating energy without the creation of carbon dioxide is required to help combat climate change and methane pyrolysis is a potential answer.

Heat and power are used almost everywhere in the world with the main uses being industrial, residential, agriculture, commercial, and in transportation. Methane pyrolysis could be used in all these applications however at very different levels of efficiency. The use of methane pyrolysis within industrial heating applications such as using the high temperature hydrogen in a boiler to generate steam instead of methane would greatly reduce carbon dioxide emissions. Industrial heating is the most economical way of using the hydrogen created by pyrolysis due to the high temperature of the hydrogen post-reaction, thus if the excess heat in the products was not utilized it would be a substantial loss in the amount of energy created. The high temperature hydrogen could also be used as a fuel for turbines. Mitsubishi is currently running a turbine that uses 30 % hydrogen and 70 % methane in Japan which produced 10 % less carbon dioxide compared to a turbine that runs on pure natural gas (Mitsubishi Power 2021). Mitsubishi is currently developing a turbine that runs on pure hydrogen and it is planned to be finished by 2025 (Mitsubishi Power 2021). The hydrogen could also be used for residential heating; however, it would not be as effective as the consumer would not be able to easily benefit from the carbon black generated from

the process. The use of methane pyrolysis in transportation (*e.g.,* hydrogen fuel cells or hydrogen internal combustion engines) is possible, however there is a small penalty in energy lost of 9 % if hydrogen is initially at 1273 K because the hydrogen product would have to be cooled for storage (9% of the total energy of hydrogen at 1273 K is thermal and would be lost if cooled to 298 K) (Cengel and Boles 2015)[1].

1.1.1 Hydrogen Production

Hydrogen is not readily available in nature and therefore must be produced from other sources such as natural gas, biomass, coal, methanol, naphtha, heavy oil, solar, wind, and water (Navarro *et al.* 2009). Current hydrogen production is split between almost 50 % steam reforming of natural gas, 30 % higher hydrocarbon reforming, 18 % from coal gasification, 3.9 % from water electrolysis, and 0.1 % from other sources (Navarro *et al.* 2015). Natural gas is the main source of hydrogen production due to the abundance of natural gas resources (Konieczny *et al.* 2008). Natural gas is also mainly made up of methane (~90 %) and methane has the highest hydrogen – carbon ratio among all hydrocarbons (Ashik *et al.* 2017).

Steam methane reforming is defined by the following reactions (Bhat and Sadhukhan 2009):

$$\text{Steam reforming: } \mathrm{CH_4} + \mathrm{H_2O} \leftrightarrow \mathrm{CO} + 3\mathrm{H_2},\ h_\mathrm{f}^\circ = 206\ \mathrm{kJ/mol} \tag{1.2}$$

$$\text{Water shift: } \mathrm{CO} + \mathrm{H_2O} \leftrightarrow \mathrm{CO_2} + \mathrm{H_2},\ h_\mathrm{f}^\circ = -41\ \mathrm{kJ/kmol} \tag{1.3}$$

$$\text{Overall reaction: } \mathrm{CH_4} + 2\mathrm{H_2O} \leftrightarrow \mathrm{CO_2} + 4\mathrm{H_2},\ h_\mathrm{f}^\circ = 164.9\ \mathrm{kJ/kmol} \tag{1.4}$$

[1]Hydrogen's chemical energy is determined from its higher heating value ($HHV = 141.795\ \mathrm{MJ/kg}$) and its thermal energy is determined from its specific heat capacity ($c_p = 14.307\ \mathrm{kJ/kgK}$) and the temperature change (1273 K – 298 K). Therefore, the percent of energy lost can be determined from: $E_{\mathrm{lost}} = \frac{c_p \Delta T}{HHV + c_p \Delta T} = 9\%$

where, h_f° is the enthalpy of formation. Methane from the natural gas reacts with steam to produce carbon monoxide and hydrogen, however, since carbon monoxide is toxic it is reacted again with steam to produce carbon dioxide and hydrogen. Steam methane reforming releases about 13.9 kg of carbon dioxide per kg of hydrogen produced (Rodat *et al.* 2009). Steam reforming is a developed technology that currently has a high hydrogen yield efficiency of ~74 % and is estimated to cost 2.27 USD/kg of hydrogen (Velazquez Abad and Dodds 2017). The main disadvantage of steam reforming is the production of carbon monoxide and carbon dioxide (Kumar and Himabindu 2019).

Higher hydrocarbon steam reforming follows the same process as natural gas reforming, and they are usually used in conjunction with one another. Higher hydrocarbons are also reformed through partial oxidation, which is the process of reacting the hydrocarbons with a small amount of air to induce incomplete combustion producing hydrogen and carbon monoxide (Speight 2015). Catalytic partial oxidation is an exothermic reaction while steam reforming is an endothermic reaction and thus catalytic partial oxidation has a higher energy efficiency when compared to stream reformation (Speight 2014). However, since the process is highly exothermic it raises issues for temperature control of the process (Speight 2014).

Coal gasification is the process of mixing an oxidizing agent, usually air or oxygen, and steam with coal at high temperatures to ignite the fuel (Thakur 2020). Coal gasification is used to produce synthesis gas (or syngas) which is a mixture of hydrogen, carbon monoxide, and carbon dioxide (Roddy and Younger 2010). This is usually done underground by injecting the oxidizing agent and steam into the coal seam to ignite the fuel underground in combination with carbon capture and storage to help reduce the environmental impact of the products (Roddy and Younger 2010). The syngas can be used as a fuel for gas turbines or for chemical synthesis (Roddy and

Younger 2010). Coal gasification has a low process energy efficiency of between 50 % and 80 % (Velazquez Abad and Dodds 2017). The main disadvantage of coal gasification is the production of carbon monoxide, carbon dioxide, and small quantities of various contaminants including sulfur oxides, nitrogen oxides, and hydrogen sulfide (Thakur 2020).

Water electrolysis is another way of producing hydrogen without the creation of carbon dioxide. It is defined by the following reactions (Chi and Yu 2018):

$$\text{Anode: } H_2O \rightarrow \frac{1}{2}O_2 + 2H^+ + 2e^- \quad (1.5)$$

$$\text{Cathode: } 2H^+ + 2e^- \rightarrow H_2 \quad (1.6)$$

$$\text{Overall: } H_2O \rightarrow H_2 + \frac{1}{2}O_2 \quad (1.7)$$

where, water is split with direct current in a two-step process that results in hydrogen and oxygen. At ambient temperature and pressure, a minimum of voltage of 1.481 V is required for electrolysis to happen and thus has a minimum energy requirement of 143 MJ/kg of hydrogen (Züttel 2004). Electrolysis is an established technology that has zero source emissions and currently has a hydrogen production efficiency of 68 % – 80 % (depending on the cell voltage, temperature, electrolyte flow conditions, and operating pressure) and is estimated to cost 3.9 USD/kg of hydrogen (Velazquez Abad and Dodds 2017). The main disadvantage of electrolysis is that the process is energy intensive and requires four times the energy to extract 1 mol of hydrogen from water when compared to hydrocarbons (Millet 2015).

1.1.2 Carbon Black Production

Methane pyrolysis also creates carbon black that can be utilized on the industrial scale as it is valuable in certain forms as a raw material for industrial uses such as rubber, ink, and pigments (Donnet *et al.* 1993). About 90 % of current carbon production is used in rubber products (Baan

et al. 2006). The annual production of carbon black is estimated at 8.1 Mt (International Carbon Black Association 2016). If 50 % of all the available natural gas in the US was converted into hydrogen and carbon black through methane decomposition an estimated 40 Mt of carbon black would be produced (Muradov and Veziroğlu 2005).

The process of making carbon black through methane decomposition is known as the thermal black process. Figure 1.1 shows the typical thermal black production process. The process uses a pair of furnaces that alternate in five-minute intervals between preheating and carbon black production (International Carbon Black Association (ICBA) 2020). The natural gas is injected into the high temperature furnace with an inert atmosphere and decomposes into hydrogen and carbon black (see equation 1.1). The product stream (containing hydrogen, carbon black, and other hydrocarbons) is quenched with water sprays and filtered (International Carbon Black Association (ICBA) 2020). The created hydrogen is then injected into the other furnace with air and burns to create heat to preheat the furnace and the residual heat can be used to generate electrical power (International Carbon Black Association (ICBA) 2020). The thermal black production process can result in a wide variety of carbon morphologies such as carbon black, graphite like carbon, coiled carbon nanotubes, multi-walled carbon nanotubes, and many others depending on the temperature and catalyst used (Keipi *et al.* 2016). There is a large price range for the carbon black produced, but it approximately has price of $300/ton or more depending on morphology (Muradov and Veziroğlu 2005).

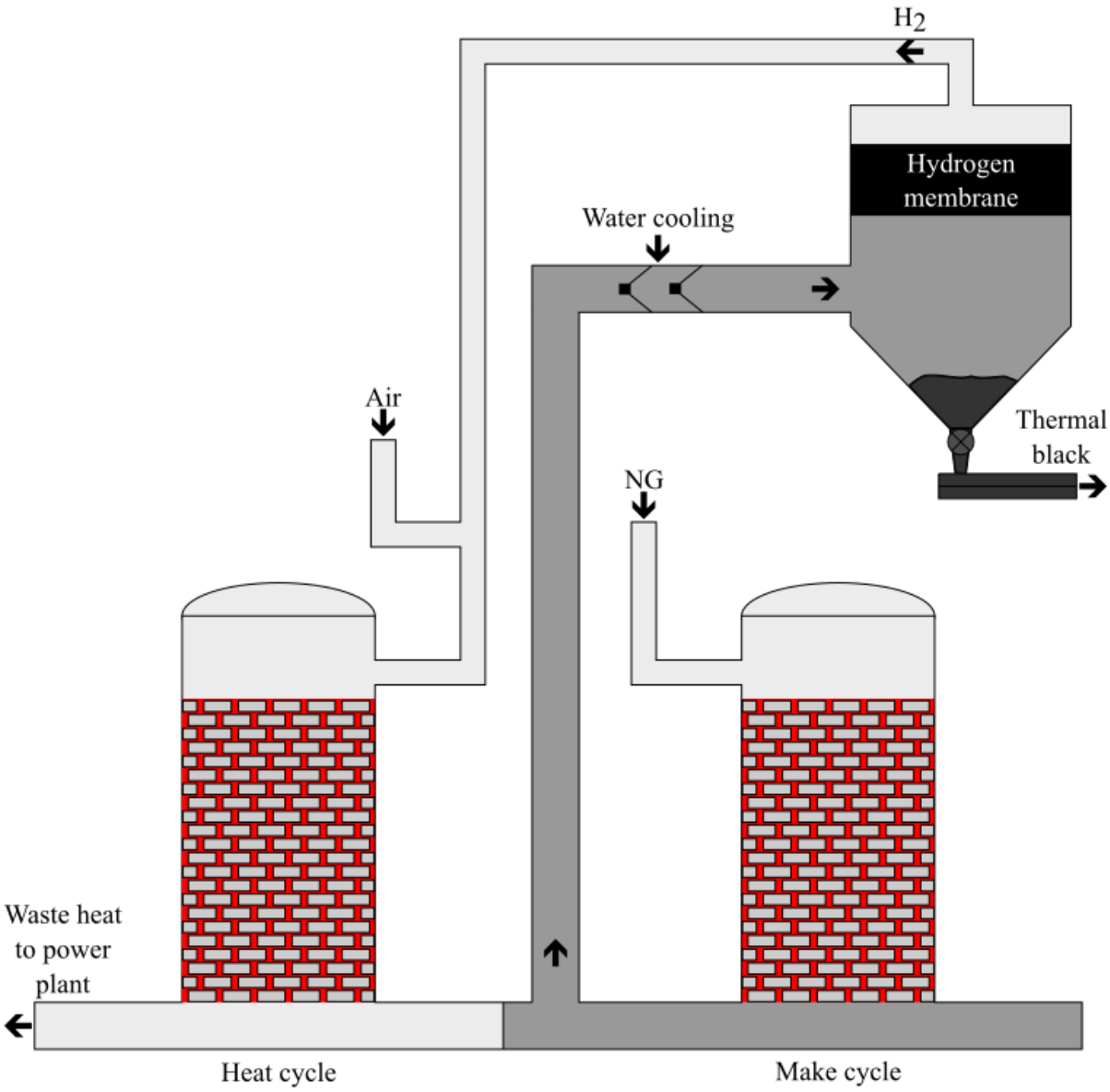

Figure 1.1: Typical thermal black production process. (Designed with reference to an image taken from International Carbon Black Association (ICBA) 2020)

Other than the thermal black production process, other methods for producing carbon black are the furnace black process, acetylene black process, and lamp black process (Long *et al.* 2013). Currently 90 % of carbon black production is from the furnace black process (Gautier *et al.* 2016). Most of the other 10 % is from the thermal black process with less than 1 % coming from the lampblack process and the acetylene black process (U.S. Environmental Protection Agency 1995).

Furnace black is based on the incomplete combustion of aromatic oils that produce carbon black, carbon dioxide, steam, and hydrogen (Fulcheri and Schwob 1995). The oils are mixed into high temperature steam where they are vaporized to form microscopic carbon particles and residual gases such as carbon monoxide and hydrogen (International Carbon Black Association 2016). The carbon black is then conveyed through the reactor where it is cooled, filtered, and collected in bags through a continuous process (International Carbon Black Association 2016). Acetylene black is the production of carbon black from acetylene. Acetylene black is made by decomposing acetylene at temperatures of 1773 K or greater (Shakourzadeh Bolouri and Amouroux 1986). Carbon black with similar properties to acetylene black can also be made using microwave plasma-catalytic reactions with methane (Cho *et al.* 2004). The acetylene black process produces carbon black with higher structures and crystallinity and is mainly used for electric conductive agents (Mitsubishi Chemical 2020). Lamp black generates carbon black by collecting the soot from the burning of oils or woods and is the oldest method for carbon black production (Mitsubishi Chemical 2020). This type of carbon black is not suitable for mass production but is used as a raw material for ink sticks for its specific color (Mitsubishi Chemical 2020).

1.2 Literature Review

In this section, the experimental methods used for methane pyrolysis are first discussed which goes into depth into the main apparatuses used.

1.2.1 Experimental methods for methane pyrolysis

Models are required to design reactors used for methane pyrolysis. However, to make accurate models reaction rates are required. Experiments are used to determine the reaction rates for different apparatuses that could be used for methane pyrolysis. There are currently three main

types of apparatuses used to determine reaction rates of methane pyrolysis: shock tubes, tube/flow reactors, and batch reactors.

1.2.1.1 Shock tubes

A shock tube is a long tube with two separate sections with different pressures with closed ends (Hanson and Davidson 2014). Shock tubes are used to create high temperatures in a localized region. This allows the compounds to react at high pressures and temperatures over very short time scales. High pressures are used so the shock tube reactions can be run at high temperatures (2000 – 3000 K) and then rapidly quenched, isolating the primary reaction products (Dahl *et al.* 2002). Shock tubes are used to replicate constant-volume reactors for short time scales (Grogan and Ihme 2017). Shock tubes can have reactions on the order of milliseconds (Dahl *et al.* 2002). Ethane and ethylene are short-lived in shock tube reactions as they quickly decompose by reactions not involving free radicals (Khan and Crynes 1970). Shock tubes are suited for determining the molecular composition in the gas phase but have difficulties when analysing particle phase products. Dust particles from the ruptured wall may also cause inhomogeneous ignition and may be a heat sink for the reaction (Grogan and Ihme 2017). They also require a large economic investment to initially set up due to the requirement of laser diagnostics to measure the species being created during the reaction due to the very short time scales.

1.2.1.2 Tube reactors

A tube reactor is an apparatus that allows the reactants to maintain a continuous motion through the system during the reaction. For example, Billaud *et al*. (1992) used a tube reactor with a length of 610 mm, internal radius of 6 mm, and an external diameter of 18 mm. They injected pure methane with a flow rate of about 15 L/h into the alumina tube and found hydrogen conversion increased with reaction time (Billaud *et al*. 1992). Tube reactors advantages are that

they are good at measuring short residence times and have minimal pressure drop across the tube. Tube reactor disadvantages are that the length required to heat and develop the tube reactors must be significantly longer than the entry length to ensure that the entry length has minimal effect on reactions. It is also difficult to measure particles in a tube reactor as the particles have a large Peclet number (Pe), on the scale of 1×10^6 – 1×10^8 which means that the advection transport rate dominated over the diffusion transport rate. This causes the particles near the center of the flow to continue with the streamlines and not be significantly affected by diffusion. Pe is expected to be of the order of unity to have radially independence of species composition and thus particles are a problem with tube reactors. This is a problem because the particle residence time will greatly vary with radial position, thus there would be a large uncertainty in residence time. Tube reactors also have a difficulty with achieving long residence times as the required length of tubing is greatly increased, or the flow rate must be very low in order to achieve long residence times, and both are inconvenient and may have additional effects on the reaction.

1.2.1.3 Batch reactors

A batch reactor is an apparatus that provides a static environment for methane pyrolysis to take place that minimizes the effect motion has on the reaction while also allowing long reaction times. Batch reactors can easily extend reaction times when compared to tube reactors and shock tubes as no physical changes are required to change reaction time. This allows batch reactors to easily analyze the effect residence time has on the species created in the reactor. Batch reactors also allow for the product gas to be easily analyzed with a wide range of diagnostic tools as the sample can be collected post-reaction. Batch reactors also have the capability of analyzing the carbon black generated during the reaction using filters. However, batch reactors have issues with filling time and the time required to heat the methane to high temperatures. The shorter the filling

time the less likely the methane is to react before reaching the vessel. The methane is also inserted at ambient temperature that is much lower than the temperature in the vessel used for heating which means that additional time is needed to heat the methane.

1.2.2 Experimental studies using batch reactors

Chen *et al.* (1975) and Chen *et al.* (1976) completed methane pyrolysis experiments in a batch reactor at temperatures of 995, 1038, 1068, and 1103 K over the absolute pressure range of 3 – 99 kPa with reaction times as long as 50 minutes. They used a quartz vessel of 478 cm^3, 20.4 cm long, and with an outer diameter of 6.0 cm for the experiments (Chen *et al.* 1975). Chen *et al.* (1975) found that hydrogen concentration increased, and methane concentration decreased as reaction time increased. They also measured an increase in concentration of ethane, ethylene, and acetylene as reaction time increased, but no acetylene was detected for reactions shorter than 25 minutes (Chen *et al.* 1975). Chen *et al.* (1976) added qualitative analysis for propylene, acetylene, allene, butadiene, and benzene not discussed in Chen *et al.* (1975). They saw an overall increase in higher hydrocarbon concentration with an increase in reaction time Chen *et al.* (1976).

Arutyunov *et al.* (1991) also completed methane pyrolysis experiments in a batch reactor at higher temperatures of 1100 – 1300 K and at multiple pressures (mainly around 59 kPa) for reaction times of 2 s – 30 minutes. They used a quartz vessel that was 100 mm long and had a diameter of 46 mm or 21 mm (Arutyunov *et al.* 1991). Arutyunov *et al.* (1991) did not measure pressure during the reaction and only measured the pressure after the specified reaction time. They used a reactant mixture that consisted of ~90 % methane and ~10 % nitrogen (Arutyunov *et al.* 1991). Arutyunov *et al.* (1991) saw an increase in hydrogen concentration and a decrease in methane concentration with an increase in reaction time. They also measured the concentration of

ethane, ethylene, and acetylene but the total concentration of these species was never seen to be above 1 %.

1.3 Contribution

There are currently few studies about methane pyrolysis inside a batch reactor and no study about methane pyrolysis at high pressures (> 100 kPa) and temperatures below 995 K. Other studies in this area such as Chen *et al.* (1975) used low pressure (3 – 99 kPa) and temperatures of 995 K – 1103 K for methane pyrolysis. Arutyunov *et al.* (1991) also investigated methane pyrolysis in a batch reactor at low pressures (15 – 93 kPa) but with a temperature range of 1100 – 1300 K. The parameters from both these studies are far different from the ones used with this project and this work aims to provide a wider range of methane pyrolysis data not yet explored. This is important because the new data points will help the kinetic model better predict the results over a wider range of temperatures and pressures. Figure 1.2 shows the temperatures and pressures used in other literature for methane pyrolysis experiments in different reactors (tube reactors and constant volume batch reactors). It shows how the experimental data collected in this work (labeled Tatum on the figure) has never been explored and would be an asset for future modeling and experimental projects.

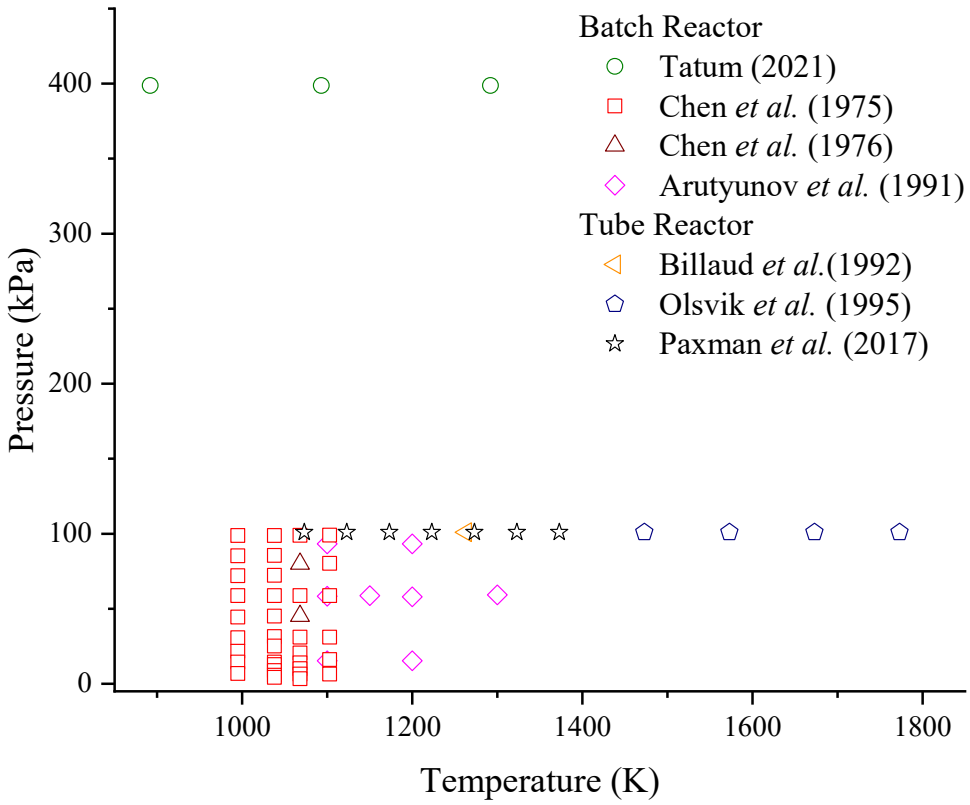

Figure 1.2: Methane pyrolysis experiments from literature (Tatum is this work).

1.4 Objectives

The goal of this thesis is to develop an experimental apparatus to determine the conversion rate and efficiency of methane conversion into hydrogen through pyrolysis inside a constant volume batch reactor at high pressures and temperatures. The apparatus was designed to allow for long residence times for methane decomposition in an oxygen-free quartz vessel while also allowing for temperature and pressure measurements. The temperature measurements were used to compare the effects temperature had on the molar concentration of hydrogen generation. The molar concentration of the products was measured using gas chromatography to determine the reaction rates at different temperatures.

1.5 Thesis outline

Chapter 2 Experimental Design, examines the experimental setup created for this project, discusses how an experiment is completed, and how the experimental results are measured. The limits of detection for the gas chromatograph are discussed as well as the uncertainty analysis for all data. Chapter 3, Results and Discussion, examines the results of this project at different oven temperatures and goes into detail about the comparison of hydrogen and methane molar concentrations in the products. Chapter 4, Conclusions and Future Work, summarizes the project and the results and discusses future work.

2 Experimental Design

The experiment was designed to investigate the effect temperature has on pyrolysis of methane inside a constant volume batch reactor.

A diagram of the experimental setup is shown in Figure 2.1. A quartz vessel (32 ml) (see Appendix A for dimensions) was placed inside an oven (Thermo Scientific Thermolyne Furnace Benchtop Muffle/Type 47900) where it was heated to high temperatures (873 – 1273 K). The vessel was connected to a series of tubes (1/8" OD & 0.069" ID 304L Stainless steel) that connects to a pressure sensor (SSI Technologies Inc. P51-100-G-B-I36-5V-000-000), two thermocouples (Omega TJ36-CAIN-116E-18), sample bag (Environmental Sampling Company 0735-7000-GD), five-way ball valve (Swagelok SS-43ZF2-049), two solenoid valves (Parker 009-0089-900), two ball valves (Swagelok SS-41GS2), filter holder (Advantec KS13 301000), filter (Advantec J010A013A) and a vacuum pump (Edwards RV12).

The experiment was run with a microcontroller (Teensy) (see Appendix B for codes used) that controls the timing of the two solenoid valves (feed and exhaust) while the other two ball valves were controlled manually. The valves voltages as well as the pressure and temperature of the system were measured using LabVIEW. The data was collected using multiple data acquisition devices (DAQ) that were connected to a chassis (National Instruments cDAQ-9178). The solenoid valves voltages were collected using NI-9223, the temperature data was collected using NI-9213, and the pressure data was collected using NI-9220. Experiments were completed with the oven setpoint at 873 K, 1073 K, and 1273 K. The regulator on the methane bottle was set to 400kPa and remained the same for all experiments. Reactions were completed with time scales of 15 s, 30 s, 60 s, 180 s, and 300 s.

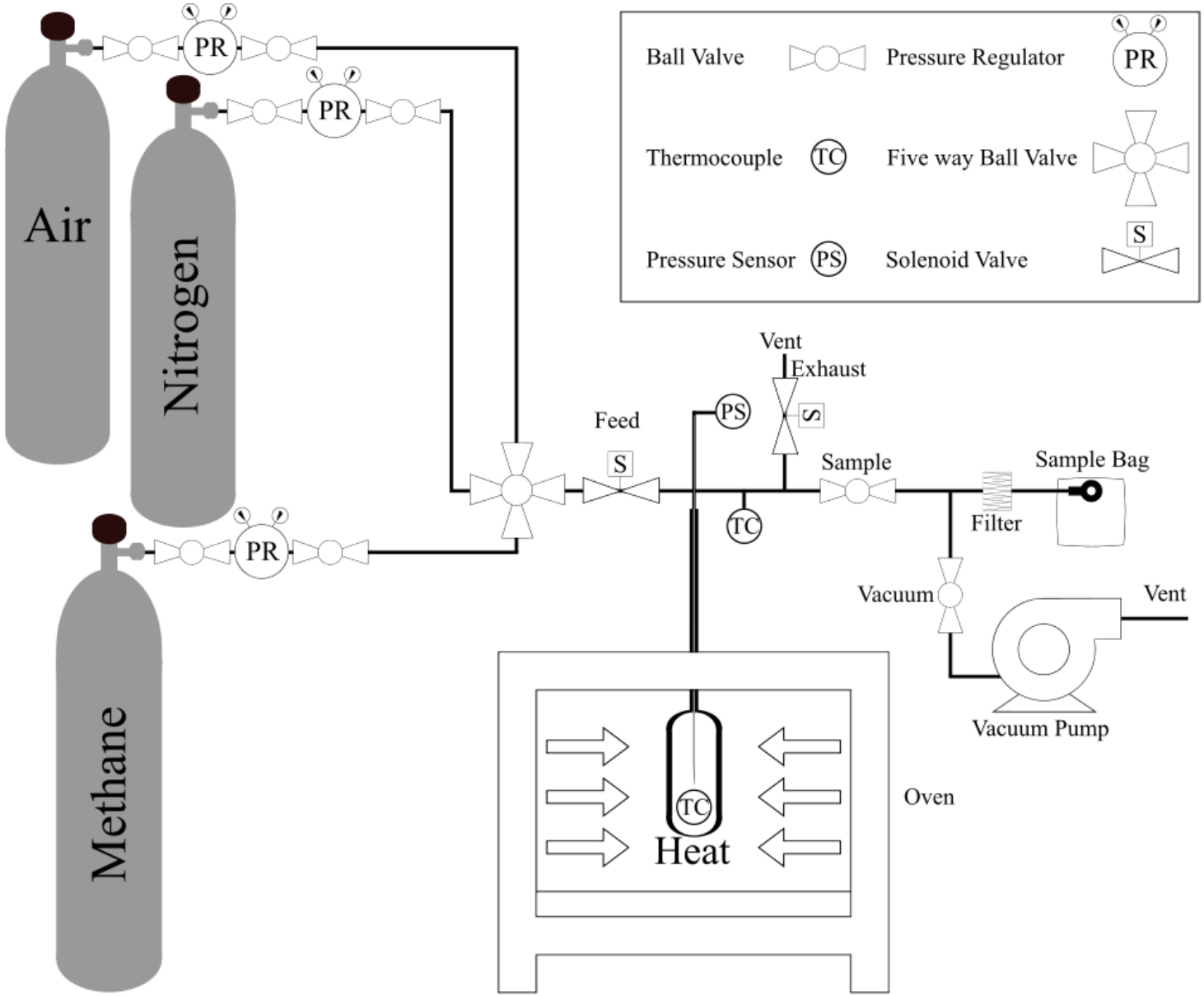

Figure 2.1: Batch reactor experimental setup used for methane pyrolysis.

2.1 Preparing the system

The sample bag valve was opened and was then attached to the setup and the system was vacuumed for 30 s with the sample valve and vacuum valve opened while the feed valve and exhaust valve were closed. The system was vacuumed to less than 0.7 kPa (the resolution of the pressure gauge was 0.7 kPa).

The five-way valve was turned to nitrogen and the system was then purged with pressurized 4.8 purity nitrogen (99.998%) at 280 kPa by opening the feed valve and closing the sample valve and vacuum valve while the exhaust valve remained closed. The feed valve remained open for ~1 s as the pressurized nitrogen quickly filled the vessel and the tubing lines as there is a large pressure differential due to the vacuum in the vessel.

The system was again vacuumed to less than 0.7 kPa for 30 s by opening the vacuum and sample valve and closing the feed valve while the exhaust valve remained closed. This ensured that little to no residual gas would be left in the vessel and if there were residual gas it would be an inert gas.

2.2 Collecting a sample

To collect a sample, the sample valve was then closed but the vacuum valve remained open to continually vacuum the sample bag during the experiment. The five-way valve was turned to methane. The feed valve was opened, and methane pressurized at 400 kPa quickly filled the vessel due to the large pressure differential. Methane was added to the vessel over a very short time (< 1 s) to ensure that the gas-exchange time was much less than the reaction time. Figure 2.2 shows an example pressure trace for an experiment as well as the temperature and pressure measured (see Section 2.6 for uncertainty details). Figure 2.2a shows an example pressure trace

during a 15 s experiment whereas Figure 2.2b shows only the first 1.5 s of the same experiment. In this example the vessel was filled to 400 kPa in ~ 0.4 s and this was typical for all experiments.

After the vessel was filled, the feed valve was closed, and the methane was left in the reactor for the desired reaction time (between 15 s to 30 min). Figure 2.2a shows there is a short constant-pressure period at the start of the experiment (labeled delay) followed by a pressure increase in the section. The pressure increase (after ~ 2 s) is due to the creation of hydrogen and intermediate species through the pyrolysis of methane (as seen in equation 1.1). The pyrolysis of methane into hydrogen doubles the moles of gases which therefore increases the pressure inside the vessel. The reaction time is labeled as reaction on Figure 2.2a.

After the reaction time had passed the exhaust valve was opened for a very short time (~ 50 ms) to purge the lines of cold unreacted gas in the tubes. The gas in the lines leaves the system because of the large pressure differential between the system at 400 kPa and atmosphere. Figure 2.2a shows the drop in pressure due to the opening of the exhaust valve in the section labeled vent. The volume of the unreacted gas was small compared to the vessel (2 ml for lines and 32 ml for the vessel) but the unreacted gases would cause an error in the conversion efficiency of the experiment. The system was therefore vented to reduce the error in the measured concentration. The vacuum valve was then closed before the sample valve was opened which released the products into the sample bag due to its lower pressure relative to the vessel. Figure 2.2a shows the delay after venting to close the vacuum and sample valve manually. A filter was placed upstream of the sample bag to collect the solid carbon created during the reaction to ensure only gases entered the sample bag. The valve on the sample bag was then closed and the sample was then moved to the gas chromatograph (GC) (see Appendix C for more details about the GC) to be analyzed; as discussed in Section 2.4.

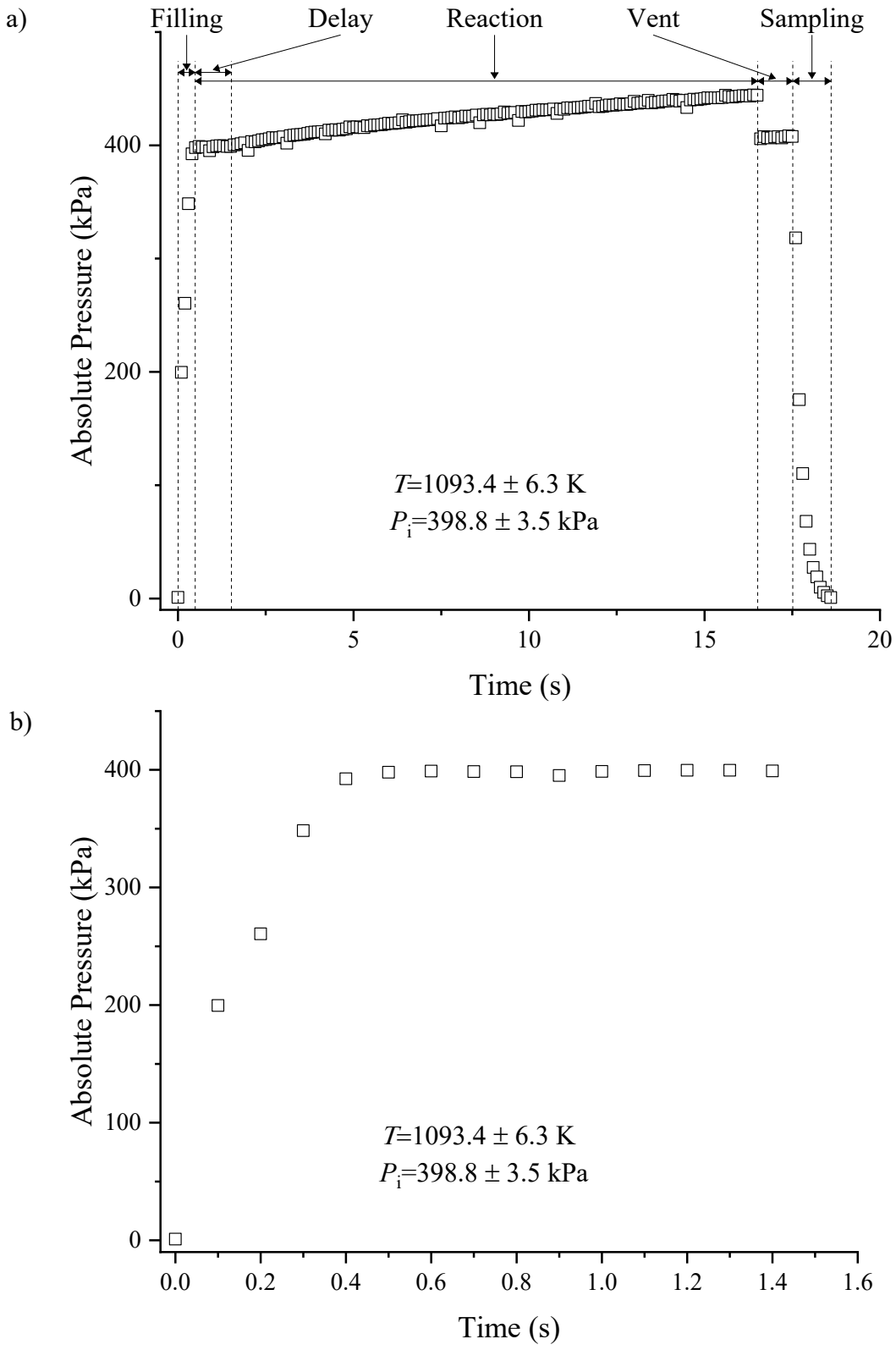

Figure 2.2:a) Pressure trace for an example reaction of 15 s b) Pressure trace to show the filling time of the system.

2.3 Cleaning the vessel

Figure 2.3 shows two images of the quartz vessel. Figure 2.3a shows the vessel after multiple experiments and Figure 2.3b shows the vessel after being cleaned. The accumulation of carbon black on the quartz vessel changes the results of the experiment depending on how much carbon accumulated on the walls of the vessel and the temperature of the experiment. The solid carbon accumulated on the vessel may lead to catalyzation of the reaction affecting subsequent experiments. These images show that the current cleaning method was sufficient in removing most if not all the carbon black coated on the vessel after a reaction.

It is believed that carbon black accumulated on the vessel serves as a radiant absorber thus catalysing the reaction further (Abanades and Flamant 2006). This means that if there was a small amount of carbon black on the walls before the start of the reaction, then there would be a higher conversion efficiency for methane. Lee *et al.* (2004) added carbon black of varying surface area and morphology to determine the effect it would have on the conversion efficiency of methane at high temperatures. All reactions completed with carbon black saw an increase in the decomposition of methane for 1223 K, 1273 K, and 1323 K (Lee *et al.* 2004). They also found that high temperature reactions (1323 K) are self-catalyzing as more carbon black is generated at the high temperatures (Lee *et al.* 2004). Lee *et al.* (2004) found that carbon black acted as a catalyst for all reactions independent of large changes to surface area and the carbon morphology.

Figure 2.4 shows the hydrogen and methane concentrations measured by the GC in repeated experiments at 899 K and 1088 K without cleaning the vessel between experiments. Figure 2.4a shows that at 899 K there was an increase in methane decomposition as more experiments were completed and thus an increase in the amount of hydrogen created. This was expected and supports literature results discussed above. However, Figure 2.4b shows that solid carbon accumulation at

1088 K led to a reduction in methane decomposition and thus a decrease in the amount of hydrogen created. This is the opposite as to what was expected for high temperature methane pyrolysis. It is unclear why higher temperatures cause solid carbon to decrease this process. For this work, we focus on clean vessel experiments. All subsequent data shown is based on measurements where the vessel was clean at the start of each experiment. Future work could look at the catalytic effect of carbon accumulation on the vessel walls.

a) b)

Figure 2.3: a) Dirty vessel after subsequent experiments b) vessel after being cleaned.

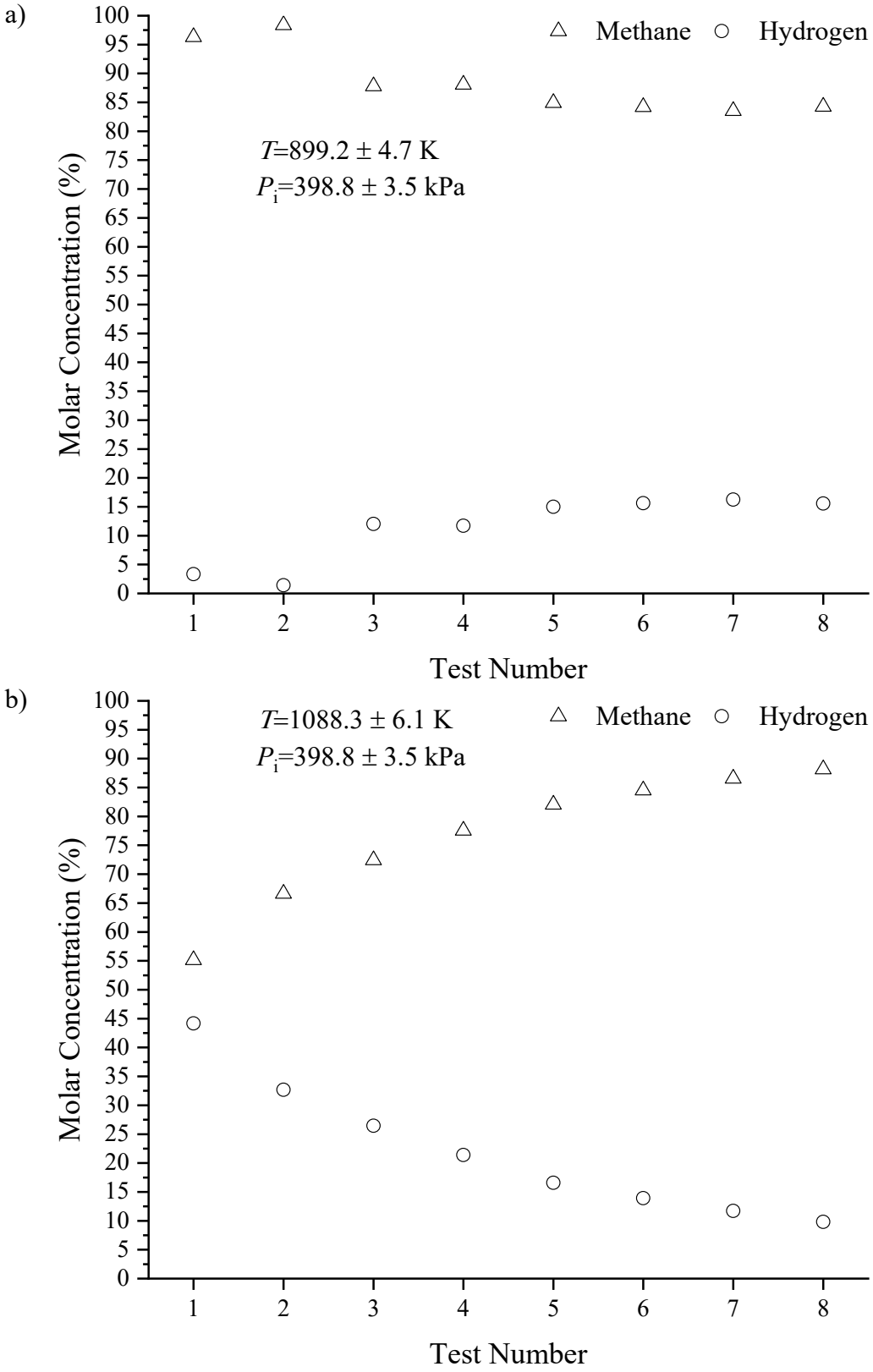

Figure 2.4: Hydrogen production as test is repeated without cleaning at a) 899 K b) 1088 K.

The vessel was cleaned by injecting air pressurized to 262 kPa into the system. This was completed by turning the five-way valve to the air line and opening the feed valve for 1 s with all other valves closed. After a reaction time of 30 s the exhaust valve was opened for 1 s to release the products into the fume hood.

It was observed that the repeatability of the experiment was related to the temperature at which the vessel was cleaned. Figure 2.5 shows pressure traces for experiments completed with the oven set at 873 K for various reaction times when cleaned with 27 cleaning cycles before each experiment. Figure 2.5a shows experiments where the vessel was cleaned at 873 K and Figure 2.5b shows experiments where the vessel was cleaned at 1073 K. Figure 2.5a shows a large discrepancy between the pressure traces for the experiments when cleaned at 873 K, whereas Figure 2.5b shows more consistent pressure traces when the vessel was cleaned at 1073 K. The pressure traces are expected to follow the same trend for all experiments completed at a given temperature if the vessel is sufficiently cleaned. Presumably, the poor repeatability observed when cleaned at 873 K is because not all the accumulated carbon was oxidized during the cleaning process. Therefore, the vessel was cleaned at a temperature of 1073 K (or higher) with 27 cleaning cycles after each experiment.

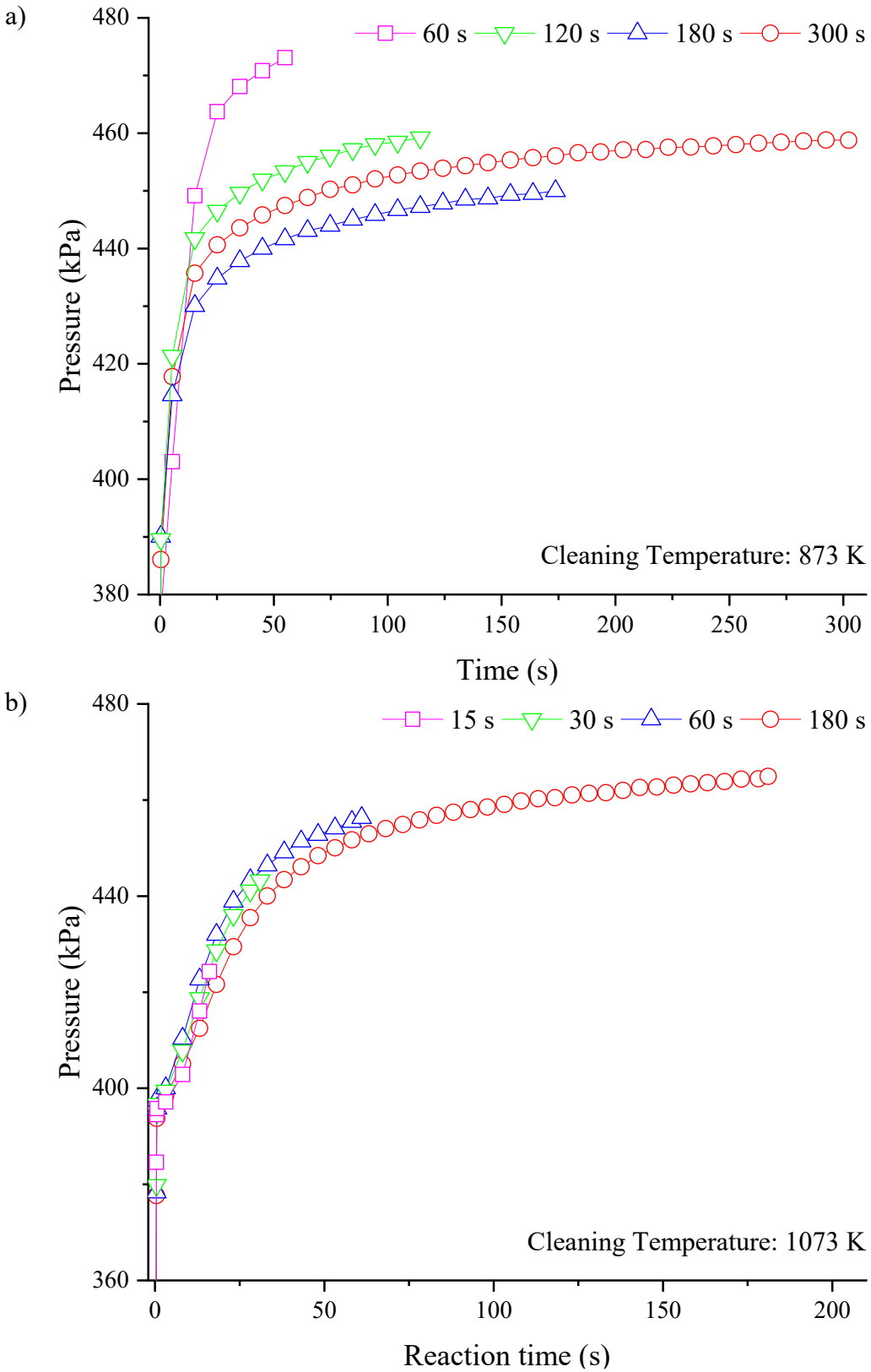

Figure 2.5: Pressure trace for experiments at an oven set point of 873 K and an initial pressure of 399 kPa when a) cleaned at 873 K b) cleaned at 1073 K after 27 cleaning cycles.

2.4 Analyzing the sample

Following the removal of the sample bag from the experimental setup the sample bag was attached to the gas chromatograph (see Appendix C for more details about the GC). Figure 2.6 shows a diagram of the GC setup. The GC was first purged with nitrogen before measuring the sample gas. Nitrogen pressurized to 280 kPa was pushed through the GC for five minutes. Following the purge, the three-way valve was then switched to the sample bag. The valve on the sample bag was then opened, and the pump was turned on for 35 s forcing the product gas to flow through the GC. The pump was then turned off and the ball valve before the pump was closed and remained closed until the pressure gauge read atmospheric pressure (to ensure the gas pressure in the GC column was at atmospheric pressure). The valve was then opened, and the GC method was run to determine the concentration of methane, ethane, ethylene, propane, acetylene, benzene, carbon dioxide, oxygen, nitrogen, carbon monoxide, and hydrogen inside the sample bag. The calibration procedure and calibration results are shown in Appendix C.

A calibration gas (49.56 % methane and 50.45% hydrogen) was run through the GC before completing any experiments to ensure that it did not have to be recalibrated (see Appendix D for details).

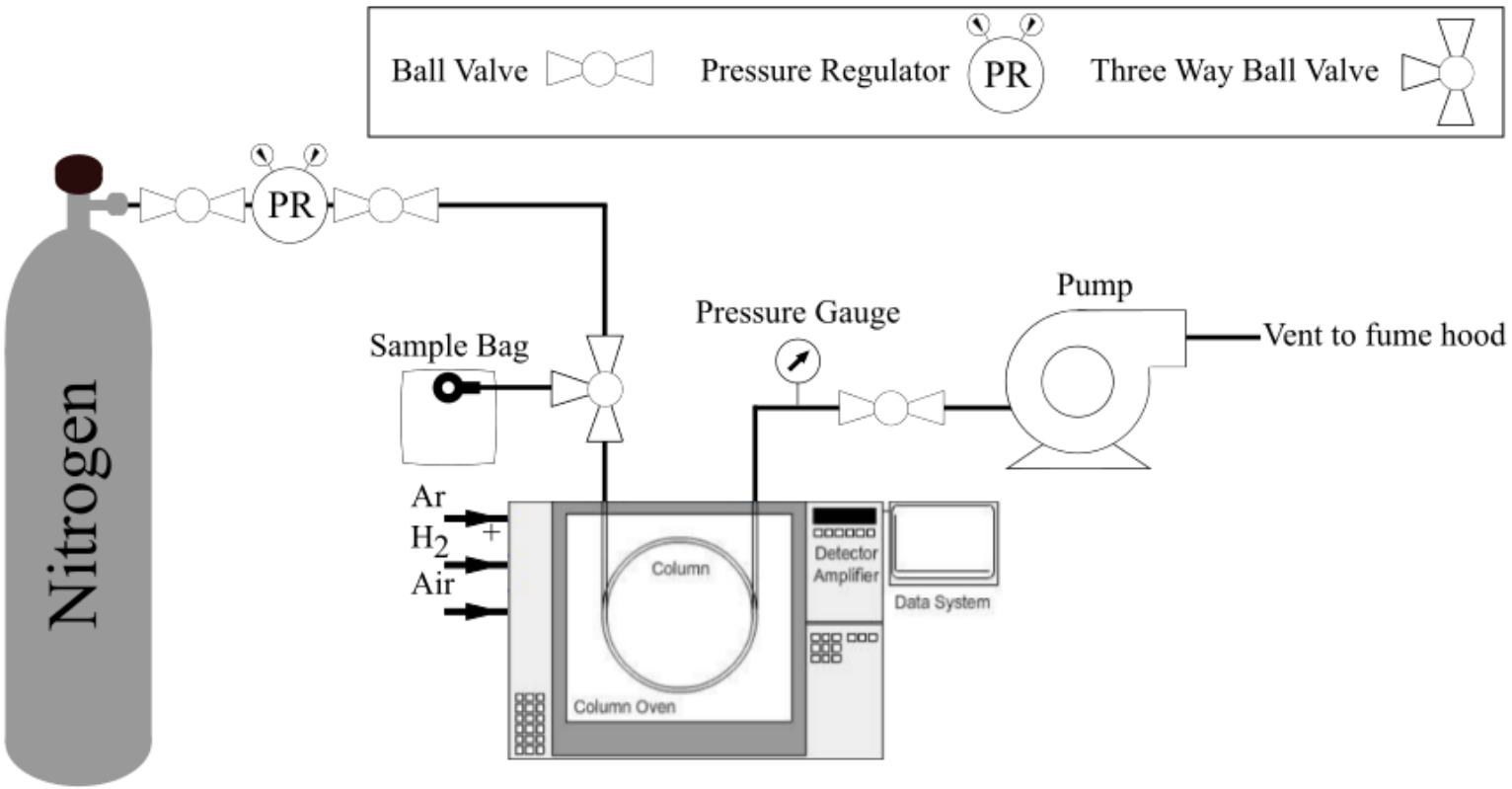

Figure 2.6: GC Setup (GC image taken from CHROMacademy 2021).

2.5 Limit of detection

There is a minimum concentration of a species that a GC can reliably detect. The limit of detection, L_{D}, is the lowest measurable concentration that can be distinguished from the noise when it is present in the sample (NCCLS 2004) and is quantified as,

$$L_{\mathrm{D}} = L_{\mathrm{B}} + 1.645\ \sigma_{\mathrm{L}} \tag{2.1}$$

where, L_{B} is the limit of blank and σ_{L} is the standard deviation of the lowest calibrated concentration of a species (Pry 2008). σ_{L} was calculated from the calibration data of the GC, specifically from calibration bottles with the lowest concentration of hydrocarbons that were used to calibrate the GC (see Appendix C for all calibration details).

The limit of blank is the highest measured concentration of a species expected to be found when there is no species present in the sample (NCCLS 2004),

$$L_{\mathrm{B}} = x_{\mathrm{blank}} + 1.645\ \sigma_{\mathrm{blank}} \tag{2.2}$$

where, x_{blank} is the mean value for all the blank concentrations, and σ_{blank} is the standard deviation of the blank concentrations (Pry 2008). x_{blank} and σ_{blank} were determined by analyzing 4.8 purity nitrogen (99.998%) with the GC. These values were orders of magnitude smaller than the calculated σ_L (>1000 times smaller) and therefore were negligible. Thus, the limit of blank is negligible in the calculation of the limit of detection.

Table 2.1 shows the L_{D}, σ_{L}, number of calibrations used, and the calibration gas concentration for the species of interest.

Table 2.1: Limit of detection for low-concentration hydrocarbons.

Species	L_D (mole %)	σ_L (mole %)	Number of Calibrations	Calibration Gas Concentration (mole %)
Ethane	1.83×10^{-5}	1.11×10^{-5}	4	0.001
Propane	2.61×10^{-5}	1.59×10^{-5}	4	0.001
Ethylene	4.20×10^{-5}	2.55×10^{-5}	3	0.00508
Acetylene	7.40×10^{-5}	4.50×10^{-5}	3	0.00512
Benzene	8.94×10^{-5}	5.44×10^{-5}	3	0.00512

2.6 Uncertainty analysis

The uncertainty in the measured concentration for each species was determined using data from multiple experiments as well as the bias uncertainty from the calibration of the GC. The total uncertainty was determined from,

$$U_x = \sqrt{{P_x}^2 + {B_x}^2} \tag{2.3}$$

where, U_x is the total uncertainty for each species, P_x is the precision uncertainty and B_x is the bias uncertainty from the calibration of the GC for each species.

The precision uncertainty is defined as,

$$P_x = t_{\propto/2,\nu}\frac{\sigma_x}{\sqrt{N}} \tag{2.4}$$

where, N is the total number of experiments, $t_{\propto/2,\nu}$ is the t-value for a confidence interval of 95%, $\propto$ is equal to one minus the confidence interval ($1 - C$, where $C = 0.95$), ν is the degrees of freedom ($N - 1$), and σ_x is the standard deviation in the measurement.

The bias uncertainty is defined as,

$$B_x = x_{\text{ave}}E \tag{2.5}$$

where, x_{ave} is the average molar concentration of the species and E is the absolute value of the maximum relative difference between the calibration gas concentration, c_{a}, and the value measured by the GC, c_{m},

$$E = \max\left\{\left|\frac{c_{\mathrm{m}_i} - c_{\mathrm{a}_i}}{c_{\mathrm{a}_i}}\right| : i = 1..n\right\} \tag{2.6}$$

Table 2.2 shows the maximum relative differences for every species measured. Appendix C shows all relative differences for all measured species.

The total uncertainty in temperature and initial pressure were also calculated the same way as above. The difference being in the calculation of bias uncertainty. The bias uncertainty for temperature was 2.2 K or 0.75% of the temperature measurement, whichever was greater. The bias uncertainty for pressure was 0.5% of full scale (100 psi) which is 3.4 kPa.

The uncertainty in time was estimated to be the time for the vacuum valve to be manually closed followed by the time for the sample valve to be manually opened after hearing the exhaust valve open. This time was estimated to be 3 s in a worst-case scenario.

Table 2.2: Maximum relative difference for the GC for every measured species.

Species	E
Helium	0.021
Hydrogen	0.0033
Methane	0.028
Ethane	0.060
Ethylene	0.059
Propane	0.046
CO2	0.053
O2	0.056
Nitrogen	0.069
Acetylene	0.105
CO	0.029
Benzene	0.060

3 Results and Discussion

Experiments were completed with the furnace set at 873 K, 1073 K, and 1273 K with the regulator on the methane bottle (99.9% methane and 0.1% helium) set at 400 kPa with the purpose to determine the reaction kinetics for methane pyrolysis at different temperatures with a fixed volume batch reactor. The actual measured temperatures inside the vessel were 892 ± 5 K, 1093 ± 6 K, and 1292 ± 8 K with an initial pressure of 399 ± 4 kPa. (The uncertainties represent 95% confidence intervals of the total uncertainty including bias and precision uncertainty as shown in Section 2.6). Multiple reaction times were analyzed at each temperature to determine the gas-phase products at each reaction time and temperature. The reaction times used were 15 s, 30 s, 60 s, 180 s, and 300 s for each temperature. The amount of solid carbon generated from the experiment was not considered as it was not possible to accurately analyze the amount of solid carbon deposited on the reactor walls.

3.1 Gas chromatography results

This section shows the results for the products analyzed with the gas chromatograph and compares it to other completed pyrolysis experiments.

3.1.1 GC results for 892 K

Figure 3.1 shows the molar concentration of products with an average measured temperature of 892 K ± 5 K inside the vessel when methane was inserted with an initial pressure of 399 ±4 kPa (for this and all other figures the uncertainties represent 95% confidence intervals of the total uncertainty including bias and precision uncertainty). Figure 3.1a shows the molar concentration of hydrogen and methane in the products. It shows that the molar concentration of hydrogen increased as the reaction time increased. The hydrogen molar concentration varied from

10.04 ± 5.85 % with a 15 s reaction time to 26.5 ± 0.81 % for a 300 s reaction time. The uncertainty in hydrogen molar concentration in the products decreased as the reaction time increased. This is expected because the uncertainty in time has a large effect on the concentration of hydrogen in the products for short reaction times and the effect is reduced as the reaction time is increased. This is because an uncertainty of 3 s for a reaction time of 15 s is large when compared to an uncertainty of 3 s for a reaction time of 300 s. The molar concentration of hydrogen also starts to plateau relative to the increase in reaction time for longer time scales. The increased production of hydrogen directly resulted in a decreased amount of methane which is expected (see equation 1.1).

Figure 3.1b shows the molar concentrations of minor species including ethane, ethylene, propane, and benzene. The error bars are large for the minor species because not all the minor species were above the lower detection limit in the products for all tests. Ethane was the only minor species that was always detected in the products at 892 K. Ethane, even though detected in every experiment, still had a large uncertainty for reaction times less than 180 s. Ethane concentrations decreased for all experiments as reaction time increased. Ethylene was detected in the products for all experiments but two (once for a 30 s reaction and once for a 60 s reaction). Ethylene also had a large uncertainty for reaction times less than 180 s. Ethylene's molar concentration in the products generally decreased as reaction time increased. Propane was only detected twice out of the 22 experiments completed (once for a 30 s reaction and once for a 60 s reaction). Acetylene was not detected for any experiments completed at 892 K and is thought to be below the lower detection limit of the GC (see section 2.5 for details of limit of detection). Benzene was only detected six times in the products for experiments at 892 K (thrice for a 300 s reaction, twice for a 60 s reaction, and once for a 30 s reaction).

Comparing these experimental results to other experiments is difficult because there are not many experimental studies for methane pyrolysis completed in batch reactors. Also, the other experimental studies were completed at different temperatures and pressures and initial conditions have a large effect on the reaction rate of methane pyrolysis. Thus, a kinetic model is needed to accurately compare the results. A kinetic model is part of a larger product that will be created using the data collected in this project as well as historical data to determine the kinetics of methane pyrolysis. Therefore, only the trends in the results of other experiments will be compared.

Chen *et al.* (1975) completed similar experiments at an initial pressure of 99 kPa and temperature of 995 K (compared to this experiment at 399 kPa and 892 K) and found that more hydrogen and less methane was detected as the reaction time increased like what was seen in this experiment. They also found that no acetylene was detected for reaction times less than 25 minutes which is similar to these results as no acetylene was detected in the products for experiments completed at 892 K (Chen *et al.* 1975). Chen *et al.* (1975) found that ethane and hydrogen were the only products at the start of a reaction for experiments completed at 995 K. However, ethylene was also detected at the start of reactions in this experiment, which was not seen by Chen *et al.* (1975) until longer reaction times. Chen *et al.* (1975) did not detect a significant amount of ethylene for reaction times shorter than 5 minutes. Table 3.1 shows all the values used to create Figure 3.1. Appendix E shows experimental results for all experiments completed.

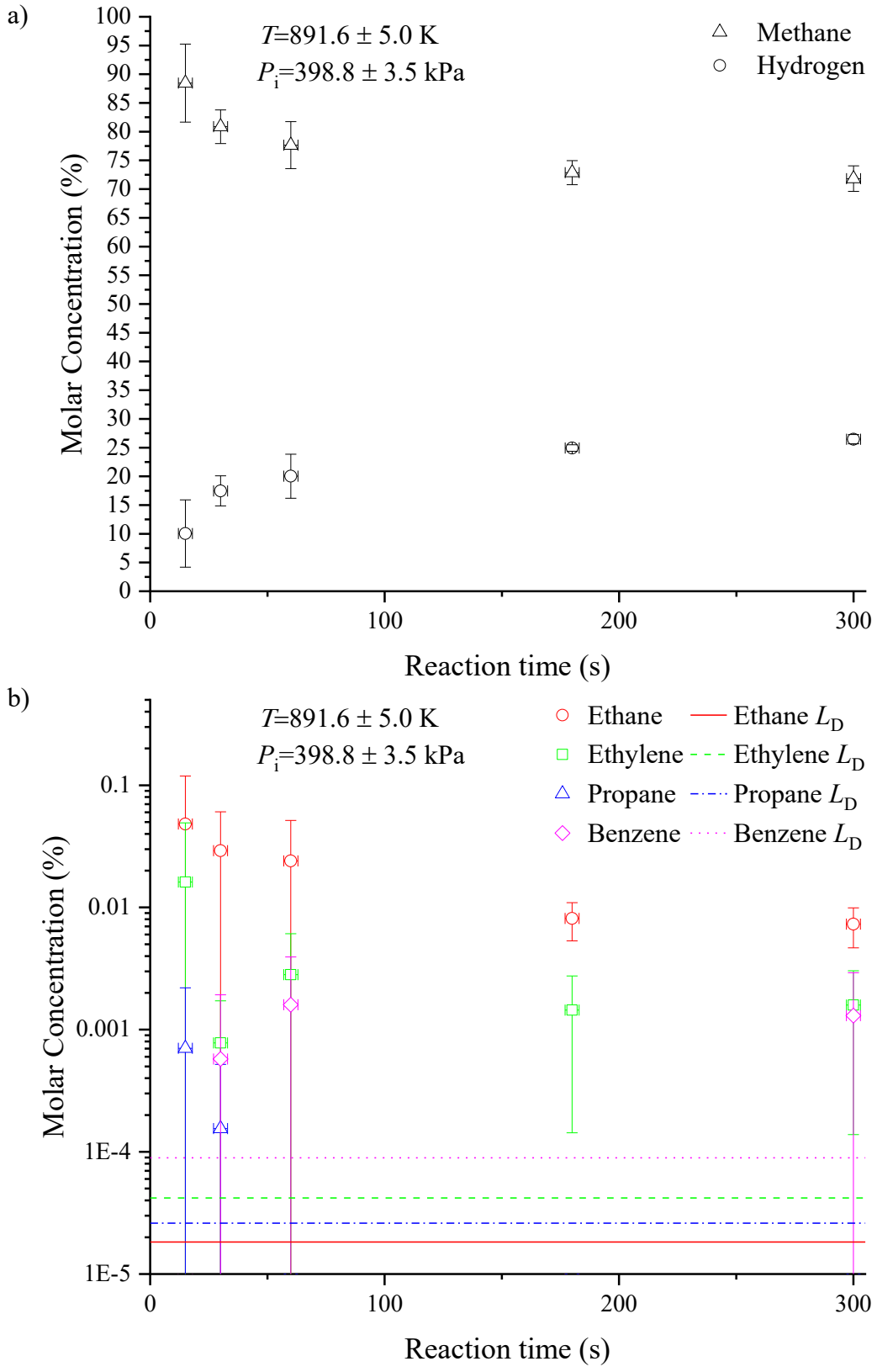

Figure 3.1: Molar concentrations for 892 K experiments with an initial pressure of 399 kPa a) Hydrogen and Methane b) Ethane, Ethylene, Propane, and Benzene.

Table 3.1: Molar concentrations for products of experiments completed at 892 K and an initial pressure of 399 kPa.

Reaction time (s)	Number of tests	CH_4 (%)	C_2H_6 (%) $x10^{-2}$	C_2H_4 (%) $x10^{-3}$	C_3H_8 (%) $x10^{-3}$	C_2H_2 (%)	C_6H_6 (%) $x10^{-3}$	H_2 (%)
15	5	88 ± 7	4.8 ± 7.0	16 ± 33	0.7 ± 1.5	ND	ND	10 ± 6
30	4	81 ± 3	2.9 ± 3.1	0.8 ± 0.9	0.2 ± 0.4	ND	0.6 ± 1.4	17 ± 3
60	3	78 ± 4	2.4 ± 2.7	2.8 ± 3.3	ND	ND	1.6 ± 2.3	20 ± 4
180	5	73 ± 2	0.8 ± 0.3	1.5 ± 1.3	ND	ND	ND	25 ± 0.6
300	5	72 ± 2	0.7 ± 0.3	1.6 ± 1.5	ND	ND	1.3 ± 1.6	26 ± 0.8

ND = not detected

3.1.2 GC results for 1093 K

Figure 3.2 shows the molar concentration of species from experiments that were completed with an average measured temperature of 1093 K ± 6 K inside the vessel when methane was inserted with an initial pressure of 399 ±4 kPa. Figure 3.2a shows the molar concentration of hydrogen and methane. It shows that the molar concentration of hydrogen increased as the reaction time increased. The hydrogen molar concentration varied from 21.75 ± 3.74 % for a 15 s reaction time to 53.0 ± 2.92 % for a 300 s reaction time. The hydrogen molar concentration for a 30 s reaction at 1093 K is comparable to a 300 s experiment at 892 K. This shows that the production of hydrogen happens much faster at 1093 K when compared to 892 K as expected since reaction rates scale with temperature.

Figure 3.2b shows the molar concentrations of ethane, ethylene, and benzene. Ethane was detected in the products for every experiment at 1093 K except for twice at a reaction time of 180 s. Ethane concentrations saw a slight decrease between reaction times until 180 s but then, had a slight increase at a reaction time of 300 s. Less ethane was detected for all experiments completed at 1093 K when compared to experiments completed at 892 K. Ethylene was detected in the products for all experiments completed at 1093 K. Ethylene saw a similar trend as ethane as its molar concentration decreased with reaction time until 180 s. Ethylene's molar concentration was

detected to be higher for a 300 s reaction time when compared to a 180 s reaction. Less ethylene was detected for all experiments completed at 1093 K when compared to experiments completed at 892 K. Propane and acetylene were not detected in the products for experiments completed at 1093 K and are thought to be below the lower detection limit of the GC. Benzene was only detected to be in the products once for all experiments completed at 1093 K (one 15 s reaction) and can be thought to otherwise be below the lower detection limit.

Chen *et al.* (1975), who conducted a similar experiment, with an initial pressure of 99 kPa and temperature of 1038 K (compared to this experiment at 399 kPa and 1093 K) saw an increase in hydrogen concentration and a decrease in methane concentration as the reaction time increased like in this experiment. Chen *et al.* (1975) also saw no acetylene production for reaction times shorter than 25 minutes which is similar to this experiment. However, Chen *et al.* (1975) saw an increased amount of ethane and ethylene for shorter time scales for experiments completed at 1038 K compared to their experiments at 995 K which is the opposite of what was seen here. Arutyunov *et al.* (1991) also completed similar methane pyrolysis experiments with a reactant mixture of 90% methane and 10% nitrogen at an initial pressure of 58 kPa and temperature of 1100 K and found a molar concentration of 18.8 % hydrogen, 70.2 % methane, and 9.05 % nitrogen after a 30-minute reaction. This is a hydrogen to methane ratio of 0.27 which is similar for experiments completed here with a reaction time of 15 s which had a hydrogen to methane ratio of 0.30. The rate of the reaction in this experiment may be faster due to the increased pressure increasing the moles of the products. Arutyunov *et al.* (1991) also found a molar concentraion of 0.71 % ethylene and 0.05 % acetylene in the same experiment. These values are both higher than the values detected in this experiment. Table 3.2 shows the data used to create Figure 3.2.

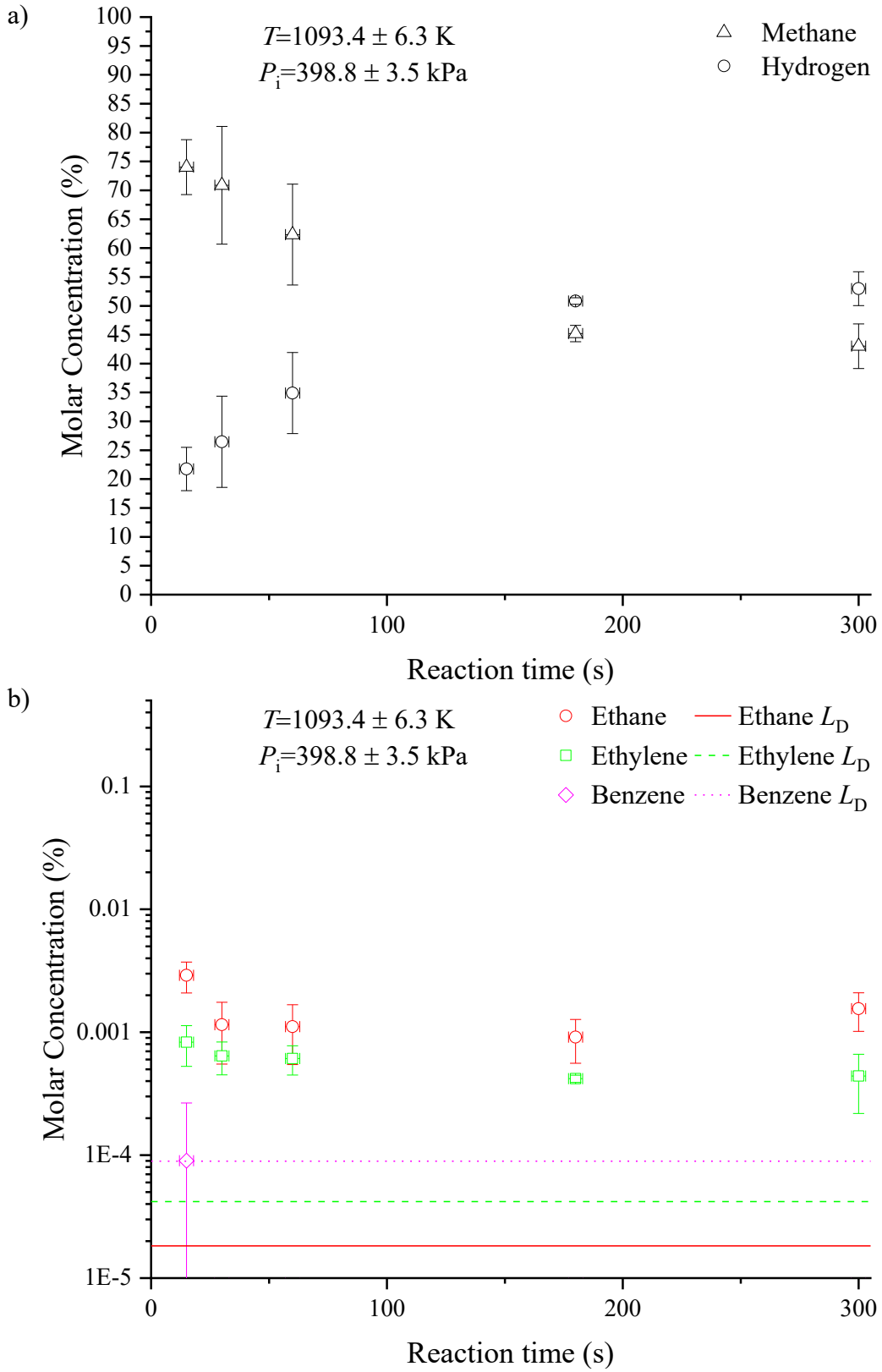

Figure 3.2: Molar concentrations for 1093 K experiments with an initial pressure of 399 kPa a) Hydrogen and Methane b) Ethane, Ethylene, and Benzene

Table 3.2: Molar concentrations for products of experiments completed at 1093 K and an initial pressure of 399 kPa.

Reaction time (s)	Number of tests	CH_4 (%)	C_2H_6 (%) $x10^{-3}$	C_2H_4 (%) $x10^{-4}$	C_3H_8 (%)	C_2H_2 (%)	C_6H_6 (%) $x10^{-4}$	H_2 (%)
15	7	74 ± 5	2.9 ± 0.8	8 ± 3	ND	ND	0.9 ± 1.8	22 ± 4
30	5	71 ± 10	1.2 ± 0.6	6 ± 2	ND	ND	ND	26 ± 8
60	7	62 ± 9	1.1 ± 0.6	6.1 ± 1.6	ND	ND	ND	35 ± 7
180	10	45 ± 1.4	0.9 ± 0.4	4.2 ± 0.3	ND	ND	ND	51 ± 0.6
300	7	43 ± 4	1.6 ± 0.5	4.4 ± 2.2	ND	ND	ND	53 ± 3

ND = not detected

3.1.3 GC results for 1292 K

Figure 3.3 shows the molar concentration of species from experiments that were completed with an average measured temperature of 1292 K ± 8 K inside the vessel when methane was inserted with an initial pressure of 399 ±4 kPa. Figure 3.3a shows the molar concentration of methane and hydrogen. It shows that the molar concentration of hydrogen increased as reaction time increased. The hydrogen molar concentration varied from 31.5 ± 1.73 % with a 15 s reaction time to 53.0 ± 2.36 % for a 300 s reaction time. The molar concentration of hydrogen for a 30 s reaction at 1292 K is comparable to a 60 s reaction at 1093 K. However, as the reaction time increased the molar concentration of hydrogen at 1093 K and 1292 K became almost identical. This shows that in this experiment there was little difference in hydrogen production at 1093 K and 1292 K for longer reaction times.

Figure 3.3b shows the molar concentrations for ethane, ethylene, acetylene, and benzene. All minor species had a higher concentration for experiments completed at 1292 K when compared to experiments completed at 1093 K. Ethane was detected in the products for every experiment at 1292 K. Ethane concentrations decreased as reaction time increased until 180 s but then, increased for the reaction time of 300 s. Experiments completed at 1292 K had a similar amount of ethane when compared to 892 K. Ethylene was detected in the products for all experiments completed at

1292 K. Ethylene followed a similar trend when compared to ethane as its molar concentration decreased as reaction time increased until 180 s. Ethylene's molar concentration was then detected to be higher for a 300 s reaction time when compared to a 180 s reaction. More ethylene was detected for all experiments completed at 1292 K when compared to experiments completed at 892 K. Propane was not detected in the products for all experiments completed at 1292 K and is thought to be below the lower detection limit of the GC. Acetylene was detected in the products for all, but four experiments completed at 1292 K (one 180 s reaction and three 300 s reactions). Acetylene again followed a similar trend when compared to ethane and ethylene as it decreased as reaction time increased until a reaction time of 180 s. Acetylene then saw a relatively large increase when compared to the other minor species for a reaction time of 300 s. Benzene was detected to be in the products for all reaction times except 180 s and one instance at 300 s for experiments completed at 1292 K. This again follows the same trend as the other detected minor species and is thought to be below the lower detection limit for experiments completed with a reaction time of 180 s.

Arutyunov *et al.* (1991) completed methane pyrolysis experiments with a reactant mixture of 90% methane and 10% nitrogen at an initial pressure of 58 kPa and temperature of 1200 K and found a molar concentration of 49.6 % hydrogen, 40.8 % methane, and 8.6% nitrogen for a reaction time of 20 minutes. This is a hydrogen to methane ratio of 1.22 which is similar to the hydrogen to methane ratio found in this experiment for a reaction time of 300 s which was 1.20. The rate of the reaction in this experiment may be faster due to the increased pressure increasing the moles of the products. Arutyunov *et al.* (1991) also found 0.02 % ethane, 0.22 % ethylene and ~0.055 % acetylene from their 20 minute experiments. These concentrations are larger than the values detected in this experiment except ethylene for short reaction times. Arutyunov *et al.* (1991)

completed similar experiments at 1300 k with the same reactant mixture and an initial pressure of 59 kPa and found a molar concentration of 79 % hydrogen and 25 % methane after a reaction time of 10 minutes. The nitrogen composition was not provided, and the summation of these values is greater than 100 % and the authors did not explain the reason for this discrepancy. The hydrogen molar concentration found at 1300 K was much greater than what was seen in this experiment at 1292 K. Arutyunov *et al.* (1991) also found no ethane, 0.26 % ethylene and ~0.12 % acetylene from this 10 minute experiment. Ethylene and acetylene concentrations are larger than the values detected in this experiment but the ethane concentration was lower as they did not detect any for reaction times greater than 20 s (Arutyunov *et al.* 1991). Table 3.3 shows all the data used to create Figure 3.3.

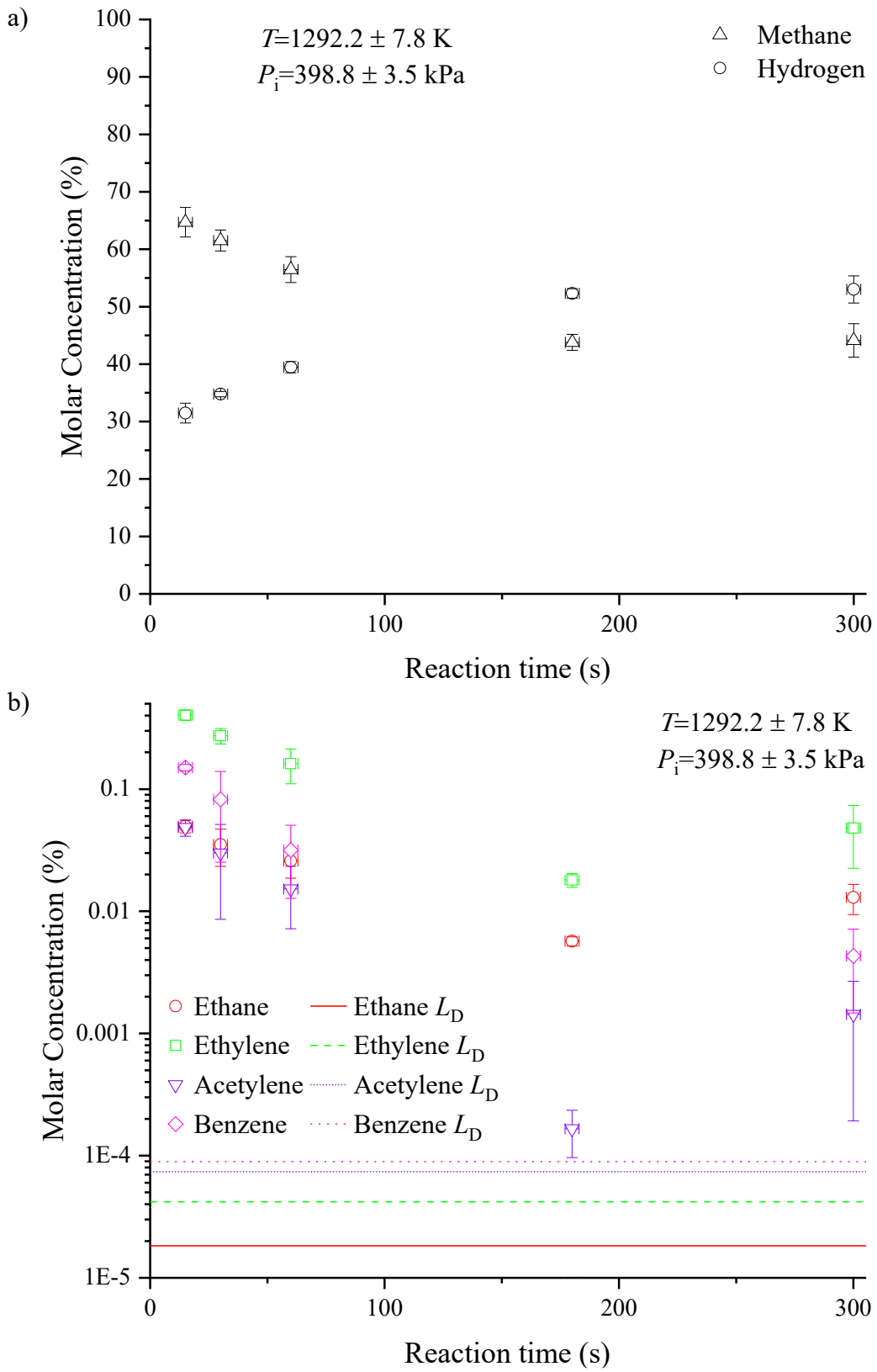

Figure 3.3: Molar concentration for 1292 K experiments with an initial pressure of 399 kPa a) Hydrogen and Methane b) Ethane, Ethylene, Acetylene, and Benzene.

Table 3.3: Molar concentrations for products of experiments completed at 1292 K and an initial pressure of 399 kPa.

Reaction time (s)	Number of tests	CH_4 (%)	C_2H_6 (%) $x10^{-2}$	C_2H_4 (%) $x10^{-2}$	C_3H_8 (%)	C_2H_2 (%) $x10^{-3}$	C_6H_6 (%) $x10^{-2}$	H_2 (%)
15	3	65 ± 3	5 ± 0.6	40 ± 4	ND	48 ± 7	15 ± 0.9	31 ± 2
30	3	62 ± 2	3.5 ± 1.1	27 ± 4	ND	30 ± 21	8 ± 6	35 ± 0.5
60	3	56 ± 2	2.6 ± 0.7	16 ± 5	ND	15 ± 8	3 ± 2	39 ± 1
180	6	44 ± 1	0.6 ± 0.05	1.8 ± 0.2	ND	0.2 ± 0.07	ND	52 ± 0.8
300	12	44 ± 3	1.3 ± 0.4	4.8 ± 2.5	ND	1.5 ± 1.2	0.4 ± 0.3	53 ± 2

ND = not detected

3.2 Comparing the pyrolysis of methane at 892 K, 1093 K, and 1292 K

The effect temperature and reaction time had on the conversion of methane into hydrogen was the focus of this experiment. Figure 3.4 shows the molar concentrations of hydrogen for experiments completed at 892 K, 1093 K, and 1292 K for reaction times of 15 s, 30 s, 60 s, 180 s, and 300 s. Figure 3.4 shows that the molar concentration of hydrogen increased significantly with an increase in temperature for experiments with reaction times less than 60 s. There was a significant increase in hydrogen molar concentration between 892 K reactions and 1093 K reactions especially for longer reaction times (180 – 300 s). However, there was only a small increase in hydrogen molar concentration between 1093 K and 1292 K experiments for longer reaction times (180 – 300 s). It requires less energy to complete experiments at lower temperatures and shorter reaction times. Thus, showing the advantages of a 1093 K experiment when compared to a 1292 K experiment even though overall more hydrogen is produced at the higher temperature. A few experiments were completed for reaction times greater than 300 s but no significant increase in hydrogen molar concentration was found.

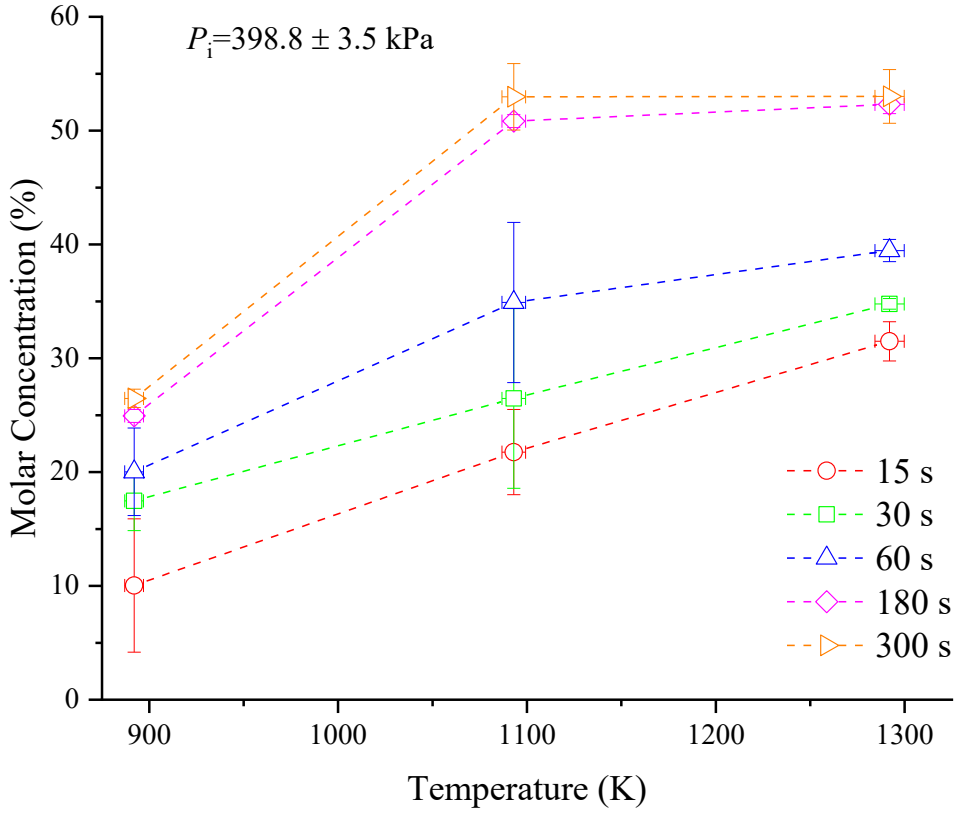

Figure 3.4: Hydrogen molar concentration for experiments with reaction times of 15, 30, 60, 180, and 300 s completed at 892 K, 1093 K, and 1292 K with an initial pressure of 399 kPa.

Figure 3.5 shows the molar concentration for methane for experiments completed at 892 K, 1093 K, and 1292 K for 15 s, 30 s, 60 s, 180 s, and 300 s. Figure 3.5 shows that methane conversion followed an inverse trend to hydrogen molar concentration. As the reaction time or temperature increased there was a decreased amount of methane present in the products. This is expected as the methane is being converted into hydrogen and solid carbon (see equation 1.1).

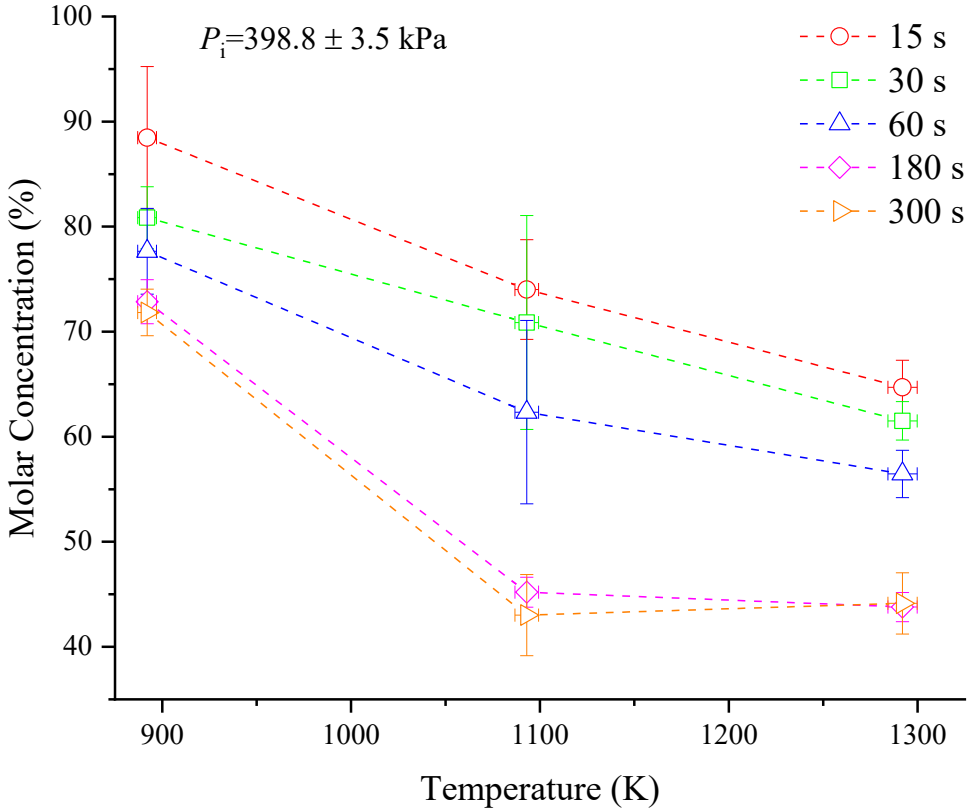

Figure 3.5: Methane molar concentration for experiments with reaction times of 15, 30, 60, 180, and 300 s completed at 892 K, 1093 K, and 1292 K with an initial pressure of 399 kPa.

4 Conclusions and Future Work

4.1 Conclusions

Pyrolysis of methane in a constant volume batch reactor was analyzed in a small-scale experimental setup. Methane pyrolysis was investigated at temperatures of 892 K, 1093 K, and 1292 K with reaction times of 15 s, 30 s, 60 s, 180 s, and 300 s with an initial pressure of 399 kPa. The molar concentration of the product gas was analyzed to determine the reaction rate at different temperatures.

Hydrogen molar concentration increased as temperature and reaction time increased. Consequently, methane concentration decreased as temperature and reaction time increased as is expected (see equation 1.1). For experiments completed at 892 K the hydrogen molar concentration varied from 10.0 ± 5.9 % with a 15 s reaction time to 26.5 ± 0.8 % for a 300 s reaction time. For experiments completed at 1093 K the hydrogen molar concentration varied from 21.8 ± 3.7 % for a 15 s reaction time to 53.0 ± 2.9 % for a 300 s reaction time. A 30 s experiment at 1093 K is comparable to a 300 s experiment at 892 K for the molar concentration of hydrogen in the products. For experiments completed at 1292 K the hydrogen molar concentration varied from 31.5 ± 1.7 % for a 15 s reaction time to 53.0 ± 2.4 % for a 300 s reaction time. A 30 s experiment at 1292 K is comparable to a 60 s experiment at 1093 K for the molar concentration of hydrogen in the products. However, for reaction times greater than 180 s and especially 300 s the molar concentration of hydrogen in the products at 1093 K and 1292 K became almost identical. Experiments completed with lower temperatures and shorter reaction times require less energy. Therefore, in certain scenarios it may be beneficial to complete experiments at 1093 K instead of 1292 K even though more hydrogen was created at 1292 K.

Minor species concentrations were the greatest for experiments completed at 1292 K when compared to 892 K and 1093 K. There was a general decrease in minor species concentration for experiments completed at 1093 K when compared to 892 K. Propane was only detected for short experiments completed at 892 K and was otherwise thought to be below the lower detection limit of the GC. Acetylene was only detected for experiments completed at 1292 K and was otherwise thought to be below the lower detection limit of the GC. Benzene, although detected for experiments at every temperature, was not consistently detected except for experiments completed at 1292 K and even then, was not detected for 180 s experiments. The summation of all minor species molar concentrations never exceeded 1 % of the species detected.

4.2 Future Work

The experiments completed only focused on the gas phase of methane pyrolysis and there is still a lot to be investigated about the solid phase. Not only the effect it had on this or similar experiments but also the quality of the solid carbon generated and how much solid carbon is generated for experiments completed at different temperatures and reaction times. The catalyzation effect solid carbon has at different temperatures could also be investigated as this experiment identified that solid carbon increased hydrogen production at lower temperatures (892 K) but decreased hydrogen production at higher temperatures (1093 K).

The following modifications/suggestions that could be investigated are:

I. Modifying initial conditions while using the same experimental apparatus

   The pressure used for these experiments was high to ensure that the fill time of the vessel was minimized so that the kinetics of the reaction could be better analyzed. The effect of different initial pressures could be investigated to see how it effects the reaction rates. The

initial concentration of methane used for experimentation could also be changed to see the effect it has on hydrogen and minor species concentrations in the products. Natural gas only consists of around 90 % methane and knowing how actual natural gas would react is important. Additional temperatures and reaction times could also be explored to expand the range of experimental data.

II. Changing the experimental apparatus

Currently there is no way to insert a physical catalyst into the vessel as it was custom made with a small entrance diameter. The effect different catalysts have on methane pyrolysis could be investigated if a vessel were made with a catalyst already inside. Carbon black also can not be efficiently measured with the current vessel due to the small entrance diameter. Changes could be made to the vessel so the carbon black could be quantified and characterized more effectively.

References

Abanades, Stephane, and Gilles Flamant. 2006. "Solar hydrogen production from the thermal splitting of methane in a high temperature solar chemical reactor." *Science Direct* 1321-1332.

Abbas, Hazzim F., and W.M.A. Wan Daud. 2010. "Hydrogen production by methane decomposition: A review." *International Journal of Hydrogen Energy* 1160-1190.

Agilent. 2021. *7890B GC System.* May 06. Accessed 07 12, 2021. https://www.agilent.com/en/product/gas-chromatography/gc-systems/7890b-gc-system.

Allen, M. R., O. P. Dube, W. Solecki, F. Aragón-Durand, W. Cramer, S. Humphreys, M. Kainuma, et al. 2018. *Framing and Context. In: Global Warming of 1.5°C. An IPCC Special Report on the impacts of global warming of 1.5°C above pre-industrial levels related global greenhouse gas emission pathways, in the context of strengthening the global response to the ...* IPCC.

Arutyunov, V. S., V. I. Vedeneev, R. I. Moshkina, and V. A. Ushakov. 1991. "Pyrolysis of methane under static conditions at 1100 - 1400 K." *Semenov Institute of Chemical Physics* 234-240.

Ashik, U.P.M., W.M.A Wan Daud, and Hazzim F. Abbas. 2015. "Production of greenhouse gas free hydrogen by thermocatalytic decomposition of methane – A review." *Renewable and Sustainable Energy Reviews* 221-256.

Ashik, U.P.M., W.M.A. Wan Daud, and Jun-ichiro Hayashi. 2017. "A review on methane transformation to hydrogen and nanocarbon: Relevance of catalyst characteristics and experimental parameters on yield." *Renewable and Sustainable Energy Reviews* 743-767.

Baan, Robert, Kurt Straif, Yann Grosse, Béatrice Secretan, Fatiha El Ghissassi, and Vincent Cogliano. 2006. "Carcinogenicity of carbon black, titanium dioxide, and talc." *The Lancet Oncology* 295-296.

Bhat, Shrikant A., and Jhuma Sadhukhan. 2009. "Process intensification aspects for steam methane reforming: An overview." *AIChE Journal* 408-422.

Billaud, F., C. Gueret, and J. Weill. 1992. "Thermal decomposition of pure methane at 1263 K. Experiments and mechanistic modelling." *Thermochimica Acta* 303-322.

Cengel, Yunus A., and Micheal A. Boles. 2015. *Thermodynamics: An Engineering Approach, Eighth Edition.* New York: McGraw-Hill Education.

Chen, C. J., M. H. Back, and R. A. Back. 1975. "The thermal decomposition of methane. i. kinetics of the primary decomposition to c2h6+ h2; rate constant for the homogeneous unimolecular dissociation of methane and its pressure dependence." *Canadian Journal of Chemistry* 3580-3590.

Chen, C.-J., M. H. Back, and R. A. Back. 1976. "The thema1 decomposition of methane. II. Secondary reactions, autocatalysis and carbon formation; non-Arrhenius behaviour in the reaction of CH3 with ethane." *Canadian Journal of Chemistry* 3175-3184.

Chi, Jun, and Hongmei Yu. 2018. "Water electrolysis based on renewable energy for hydrogen production." *Chinese Journal of Catalysis* 390-394.

Cho, Wonihl, Seung-Ho Lee, Woo-Sung Ju, Youngsoon Baek, and Joong Kee Lee. 2004. "Conversion of natural gas to hydrogen and carbon black by plasma and application of plasma carbon black." *Catalysis Today* 633-638.

CHROMacademy. 2021. "Theory and Instrumentation of GC Introduction." *moam.info.* 02 10. https://moam.info/theory-and-instrumentation-of-gc-introduction-chromacademy_599aa5ae1723dd0b40ac4a92.html.

Dahl, Jaimee K., Victor H. Barocas, Dasvid E. Clough, and Alan W. Weimer. 2002. "Intrinsic kinetics for rapid decomposition of methane in an aerosol flow reactor." *International Journal of Hydrogen Energy* 377-386.

Donnet, J. B., R. C. Bansal, and M. J. Wang. 1993. *Carbon Black Science and Technology (2nd ed.).* New York: Marcel Dekker.

Falahati, Fajad. 2018. *Experimental study of methane decarbonization to produce hydrogen using a laminar premixed flame.* MSc. Thesis, Edmonton: University of Alberta.

Fulcheri, L., and Y. Schwob. 1995. "From methane to hydrogen, carbon black and water." *International Journal of Hydrogen Energy* 197-202.

Gautier, Maxime, Vandad Rohani, Laurent Fulcheri, and Juan Pablo Trelles. 2016. "Influence of temperature and pressure on carbon black size distribution during allothermal cracking of methane." *Aerosol Science and Technology* 26-40.

Grogan, Kevin P., and Matthias Ihme. 2017. "Regimes describing shock boundary layer interaction and ignition in shock tubes." *Proceedings of the Combustion Institute* 2927-2935.

Hanson, R. K., and D. F. Davidson. 2014. "Recent advances in laser absorption and shock tube methods for studies of combustion chemistry." *Progress in Energy and Combustion Science* 103-114.

International Carbon Black Association (ICBA). 2020. "Cancarb." *Carbon Black User's Guide.* May 06. Accessed July 15, 2021. https://cancarb.com/wp-content/uploads/2020/05/carbon-black-user-guide.pdf.

International Carbon Black Association. 2016. *What is Carbon Black?* Accessed 07 15, 2021. http://www.carbon-black.org/index.php/what-is-carbon-black.

IPCC. 2014. *Climate Change 2014: Mitigation of Climate Change. Contribution of Working Group III to the Fifth Assessment Report of the Intergovernmental Panel on Climate Change.* Environmental report, Cambridge: Cambridge University Press.

IPCC. 2014. *Climate Change 2014: Synthesis Report. Contribution of Working Groups I, II and III to the Fifth Assessment Report of the Intergovernmental Panel on Climate Change.* Geneva, Switzerland: IPCC.

Keipi, Tiina, Katariina E.S. Tolvanen, Henrik Tolvanen, and Jukka Konttinen. 2016. "Thermo-catalytic decomposition of methane: The effect of reaction parameters on process design and the utilization possibilities of the produced carbon." *Energy Conversion and Management* 923-934.

Khan, M. S., and Billy L. Crynes. 1970. "Survey of Recent Methane Pyrolysis Literature." *Industrial and Engineering Chemistry* 54-59.

Konieczny, A., K. Mondal, T. Wiltowski, and P. Dydo. 2008. "Catalyst development for thermocatalytic decomposition of methane to hydrogen." *International Journal of Hydrogen Energy* 264-272.

Kumar, S. Shiva, and V. Himabindu. 2019. "Hydrogen production by PEM water electrolysis – A review." *Materials Science for Energy Technologies* 442-454.

Lee, Eun Kyoung, Sang Yeob Lee, Gui Young Han, Byung Kwon Lee, Tae-Jin Lee, Jin Hyuk Jun, and Ki June Yoon. 2004. "Catalytic decomposition of methane over carbon blacks for CO2-free hydrogen production." *Science Direct* 2641-2648.

Long, Christopher M., Marc A. Nascarella, and Peter A. Valberg. 2013. "Carbon black vs. black carbon and other airborne materials containing elemental carbon: Physical and chemical distinctions." *Environmental Pollution* 271-286.

Millet, P. 2015. "9 - Hydrogen production by polymer electrolyte membrane water electrolysis." *Compendium of Hydrogen Energy* 255-286.

Mitsubishi Chemical. 2020. *Manufacturing Process of Carbon Black.* December 17. Accessed July 15, 2021. http://www.carbonblack.jp/en/cb/seizou.html.

Mitsubishi Power. 2021. "Turbines driven purely by hydrogen in the pipeline." *Nature Portfolio.* July 10. Accessed 07 14, 2021. https://www.nature.com/articles/d42473-020-00545-7.

Muradov, N. Z., and T. N. Veziroğlu. 2005. "From hydrocarbon to hydrogen–carbon to hydrogen economy." *International Journal of Hydrogen Energy* 225-237.

Navarro, R. M., M. C. Sánchez-Sánchez, M. C. Alvarez-Galvan, J. L. G. Fierro, and F. del Valle. 2009. "Hydrogen production from renewable sources: biomass and photocatalytic opportunities." *Energy and Environmental Science* 35-54.

Navarro, R. M., R. Guil, and J. L.G. Fierro. 2015. "Introduction to hydrogen production." *Compendium of Hydrogen Energy* 21-61.

NCCLS. 2004. "Protocols for Determination of Limits of Detection and Limits of Quantitation; Approved Guideline." *NCCLS document EP17-A [ISBN 1-56238-551-8]. NCCLS, 940 West Valley Road, Suite.*

Olsvik, Ola, Odd A. Rokstad, and Anders Holmen. 1995. "Pyrolysis of methane in the presence of hydrogen." *Chemical Engineering & Technology* 349-358.

Paxman, D., S. Trottier, M. R. Flynn, L. Kostiuk, and M. Secanell. 2017. "Experimental and numerical analysis of a methane thermal decomposition reactor." *International Journal of Hydrogen Energy* 25166-25184.

Pry, David A Armbruster and Terry. 2008. "Limit of Blank, Limit of Detection and Limit of Quantitation." *The Clinical Biochemist – Reviews* S49-S52.

Riley, Jarrett, Chris Atallah, Ranjani Siriwardane, and Robert Stevens. 2021. "Technoeconomic analysis for hydrogen and carbon Co-Production via catalytic pyrolysis of methane." *International Journal of Hydrogen Energy* 20338-20358.

Rodat, Sylvain, Stéphane Abanades, Jean-Louis Sans, and Gilles Flamant. 2009. "Hydrogen production from solar thermal dissociation of natural gas: development of a 10 kW solar chemical reactor prototype." *Solar Energy* 1599-1610.

Roddy, Dermot J., and Paul L. Younger. 2010. "Underground coal gasification with CCS: a pathway to decarbonising industry." *Energy & Environmental Science* 400-407.

Sánchez-Bastardo, Nuria, Robert Schlögl, and Holger Ruland. 2020. "Methane Pyrolysis for CO2-Free H2 Production: A Green Process to Overcome Renewable Energies Unsteadiness." *Chemie Ingenieur Technik* (Chemie Ingenieur Technik) 1596-1609.

Shakourzadeh Bolouri, K., and J. Amouroux. 1986. "Reactor Design and Energy Concepts for a Plasma Process of Acetylene Black Production." *Plasma Chemistry and Plasma Processing* 335-348.

Speight, J. G. 2015. "6 - Gasification processes for syngas and hydrogen production." *Gasification for Synthetic Fuel Production* 119-146.

Speight, James G. 2014. "Chapter 5 - The Fischer–Tropsch Process." *Gasification of Unconventional Feedstocks* 118-134.

Thakur, Pramod. 2020. "20 - CO2 sequestration and underground coal gasification with horizontal wells." *Coal Bed Methane (Second Edition)* 319-333.

U.S. Environmental Protection Agency. 1995. *AP 42, Fifth Edition, Volume I Chapter 6: Organic Chemical Process Industry.* Compilation of Air Pollutant Emission Factors, North Carolina: U.S. Environmental Protection Agency, 6.1-1-6.1-10.

Velazquez Abad, A., and P.E. Dodds. 2017. "Production of Hydrogen." *Encyclopedia of Sustainable Technologies* 293-304.

Züttel, Andreas. 2004. "Hydrogen storage methods." *Naturwissenschaften* 157-172.

Appendix A Drawings

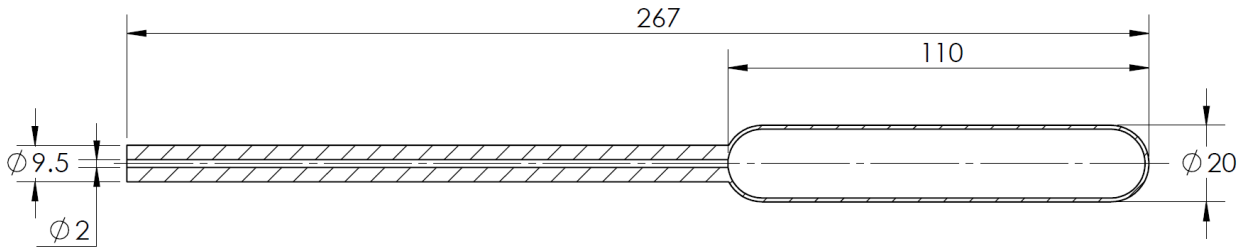

Figure A.1: Quartz vessel dimensions (all dimensions are in mm).

Appendix B Arduino Codes

B.1 Running the experiment

```
int Valve_Feed = 13;
int Valve_Vent = 14;
int Valve_Sample = 15;
int Valve_Vacuum = 23;
// the setup routine runs once when you press reset:
void setup() {
  // initialize the digital pin as an output.
  pinMode(Valve_Feed, OUTPUT);
  digitalWrite(Valve_Feed,LOW);
    pinMode(Valve_Sample, OUTPUT);
  digitalWrite(Valve_Sample,LOW);
  pinMode(Valve_Vent, OUTPUT);
  digitalWrite(Valve_Vent,LOW);
  pinMode(Valve_Vacuum, OUTPUT);
  digitalWrite(Valve_Vacuum,LOW);
digitalWrite(Valve_Vacuum, HIGH);   // turn the valve on (HIGH is the voltage
level)
digitalWrite(Valve_Sample, HIGH);   // turn the valve on (HIGH is the voltage
level)
delay(25000);                // wait for a second
digitalWrite(Valve_Sample, LOW);    // turn the valve off by making the
voltage LOW
digitalWrite(Valve_Feed, HIGH);   // turn the valve on (HIGH is the voltage
level)
delay(1500);                // wait for a second
digitalWrite(Valve_Feed, LOW);    // turn the valve off by making the voltage
LOW
delay(295000);                // reaction time
digitalWrite(Valve_Vacuum, LOW);    // turn the valve off by making the
voltage LOW
delay(5000);                // wait for a second
digitalWrite(Valve_Vent, HIGH);   // turn the valve on (HIGH is the voltage
level)
delay(5);               // wait for a second
digitalWrite(Valve_Vent, LOW);    // turn the valve off by making the voltage
LOW
 digitalWrite(Valve_Sample, HIGH);   // turn the valve on (HIGH is the voltage
level)
delay(3000);                // wait for a second
digitalWrite(Valve_Sample, LOW);    // turn the valve off by making the
voltage LOW
 // the loop routine runs over and over again forever:
void loop() {}
```

B.2 Burning off the vessel – 1 time

```
int Valve_Feed = 13;
int Valve_Vent = 14;
int Valve_Sample = 15;
int Valve_Vacuum = 23;
```

```
// the setup routine runs once when you press reset:
void setup() {
  // initialize the digital pin as an output.
  pinMode(Valve_Feed, OUTPUT);
  digitalWrite(Valve_Feed,LOW);
    pinMode(Valve_Sample, OUTPUT);
  digitalWrite(Valve_Sample,LOW);
  pinMode(Valve_Vent, OUTPUT);
  digitalWrite(Valve_Vent,LOW);
  pinMode(Valve_Vacuum, OUTPUT);
  digitalWrite(Valve_Vacuum,LOW);
digitalWrite(Valve_Feed, HIGH);    // turn the valve on (HIGH is the voltage
level)
delay(1500);                 // wait for a second
digitalWrite(Valve_Feed, LOW);    // turn the valve off by making the voltage
LOW
delay(30000);                 // reaction time
digitalWrite(Valve_Vent, HIGH);    // turn the valve on (HIGH is the voltage
level)
delay(1000);                 // wait for a second
digitalWrite(Valve_Vent, LOW);    // turn the valve off by making the voltage
LOW
// the loop routine runs over and over again forever:
void loop() {}
```

B.3 Burning off – cycle

```
int Valve_Feed = 13;
int Valve_Vent = 14;
int Valve_Sample = 15;
int Valve_Vacuum = 23;
// the setup routine runs once when you press reset:
void setup() {
  // initialize the digital pin as an output.
  pinMode(Valve_Feed, OUTPUT);
  digitalWrite(Valve_Feed,LOW);
    pinMode(Valve_Sample, OUTPUT);
  digitalWrite(Valve_Sample,LOW);
  pinMode(Valve_Vent, OUTPUT);
  digitalWrite(Valve_Vent,LOW);
  pinMode(Valve_Vacuum, OUTPUT);
  digitalWrite(Valve_Vacuum,LOW);
digitalWrite(Valve_Feed, HIGH);   // turn the valve on (HIGH is the voltage
level)
delay(1500);                 // wait for a second
digitalWrite(Valve_Feed, LOW);    // turn the valve off by making the voltage
LOW
delay(30000);                 // reaction time
digitalWrite(Valve_Vent, HIGH);   // turn the valve on (HIGH is the voltage
level)
delay(1000);                 // wait for a second
digitalWrite(Valve_Vent, LOW);    // turn the valve off by making the voltage
LOW
delay(3000);                 // reaction time
digitalWrite(Valve_Feed, HIGH);   // turn the valve on (HIGH is the voltage
level)
delay(1500);                 // wait for a second
```

```
digitalWrite(Valve_Feed, LOW);    // turn the valve off by making the voltage
LOW
delay(30000);                // reaction time
digitalWrite(Valve_Vent, HIGH);   // turn the valve on (HIGH is the voltage
level)
delay(1000);                // wait for a second
digitalWrite(Valve_Vent, LOW);    // turn the valve off by making the voltage
LOW
delay(3000);                // reaction time
digitalWrite(Valve_Feed, HIGH);   // turn the valve on (HIGH is the voltage
level)
delay(1500);                // wait for a second
digitalWrite(Valve_Feed, LOW);    // turn the valve off by making the voltage
LOW
delay(30000);                // reaction time
digitalWrite(Valve_Vent, HIGH);   // turn the valve on (HIGH is the voltage
level)
delay(1000);                // wait for a second
digitalWrite(Valve_Vent, LOW);    // turn the valve off by making the voltage
LOW
delay(3000);                // reaction time
digitalWrite(Valve_Feed, HIGH);   // turn the valve on (HIGH is the voltage
level)
delay(1500);                // wait for a second
digitalWrite(Valve_Feed, LOW);    // turn the valve off by making the voltage
LOW
delay(30000);                // reaction time
digitalWrite(Valve_Vent, HIGH);   // turn the valve on (HIGH is the voltage
level)
delay(1000);                // wait for a second
digitalWrite(Valve_Vent, LOW);    // turn the valve off by making the voltage
LOW
delay(3000);                // reaction time
digitalWrite(Valve_Feed, HIGH);   // turn the valve on (HIGH is the voltage
level)
delay(1500);                // wait for a second
digitalWrite(Valve_Feed, LOW);    // turn the valve off by making the voltage
LOW
delay(30000);                // reaction time
digitalWrite(Valve_Vent, HIGH);   // turn the valve on (HIGH is the voltage
level)
delay(1000);                // wait for a second
digitalWrite(Valve_Vent, LOW);    // turn the valve off by making the voltage
LOW
delay(3000);                // reaction time
digitalWrite(Valve_Feed, HIGH);   // turn the valve on (HIGH is the voltage
level)
delay(1500);                // wait for a second
digitalWrite(Valve_Feed, LOW);    // turn the valve off by making the voltage
LOW
delay(30000);                // reaction time
digitalWrite(Valve_Vent, HIGH);   // turn the valve on (HIGH is the voltage
level)
delay(1000);                // wait for a second
digitalWrite(Valve_Vent, LOW);    // turn the valve off by making the voltage
LOW
delay(3000);                // reaction time
```

```
digitalWrite(Valve_Feed, HIGH);   // turn the valve on (HIGH is the voltage
level)
delay(1500);               // wait for a second
digitalWrite(Valve_Feed, LOW);    // turn the valve off by making the voltage
LOW
delay(30000);               // reaction time
digitalWrite(Valve_Vent, HIGH);   // turn the valve on (HIGH is the voltage
level)
delay(1000);               // wait for a second
digitalWrite(Valve_Vent, LOW);    // turn the valve off by making the voltage
LOW
delay(3000);               // reaction time
digitalWrite(Valve_Feed, HIGH);   // turn the valve on (HIGH is the voltage
level)
delay(1500);               // wait for a second
digitalWrite(Valve_Feed, LOW);    // turn the valve off by making the voltage
LOW
delay(30000);               // reaction time
digitalWrite(Valve_Vent, HIGH);   // turn the valve on (HIGH is the voltage
level)
delay(1000);               // wait for a second
digitalWrite(Valve_Vent, LOW);    // turn the valve off by making the voltage
LOW
delay(3000);               // reaction time
digitalWrite(Valve_Feed, HIGH);   // turn the valve on (HIGH is the voltage
level)
delay(1500);               // wait for a second
digitalWrite(Valve_Feed, LOW);    // turn the valve off by making the voltage
LOW
delay(30000);               // reaction time
digitalWrite(Valve_Vent, HIGH);   // turn the valve on (HIGH is the voltage
level)
delay(1000);               // wait for a second
digitalWrite(Valve_Vent, LOW);    // turn the valve off by making the voltage
LOW
delay(3000);               // reaction time
digitalWrite(Valve_Feed, HIGH);   // turn the valve on (HIGH is the voltage
level)
delay(1500);               // wait for a second
digitalWrite(Valve_Feed, LOW);    // turn the valve off by making the voltage
LOW
delay(30000);               // reaction time
digitalWrite(Valve_Vent, HIGH);   // turn the valve on (HIGH is the voltage
level)
delay(1000);               // wait for a second
digitalWrite(Valve_Vent, LOW);    // turn the valve off by making the voltage
LOW
delay(3000);               // reaction time
digitalWrite(Valve_Feed, HIGH);   // turn the valve on (HIGH is the voltage
level)
delay(1500);               // wait for a second
digitalWrite(Valve_Feed, LOW);    // turn the valve off by making the voltage
LOW
delay(30000);               // reaction time
digitalWrite(Valve_Vent, HIGH);   // turn the valve on (HIGH is the voltage
level)
delay(1000);               // wait for a second
```

```
digitalWrite(Valve_Vent, LOW);    // turn the valve off by making the voltage
LOW
delay(3000);                 // reaction time
digitalWrite(Valve_Feed, HIGH);   // turn the valve on (HIGH is the voltage
level)
delay(1500);                 // wait for a second
digitalWrite(Valve_Feed, LOW);    // turn the valve off by making the voltage
LOW
delay(30000);                 // reaction time
digitalWrite(Valve_Vent, HIGH);   // turn the valve on (HIGH is the voltage
level)
delay(1000);                 // wait for a second
digitalWrite(Valve_Vent, LOW);    // turn the valve off by making the voltage
LOW
delay(3000);                 // reaction time
digitalWrite(Valve_Feed, HIGH);   // turn the valve on (HIGH is the voltage
level)
delay(1500);                 // wait for a second
digitalWrite(Valve_Feed, LOW);    // turn the valve off by making the voltage
LOW
delay(30000);                 // reaction time
digitalWrite(Valve_Vent, HIGH);   // turn the valve on (HIGH is the voltage
level)
delay(1000);                 // wait for a second
digitalWrite(Valve_Vent, LOW);    // turn the valve off by making the voltage
LOW
delay(3000);                 // reaction time
digitalWrite(Valve_Feed, HIGH);   // turn the valve on (HIGH is the voltage
level)
delay(1500);                 // wait for a second
digitalWrite(Valve_Feed, LOW);    // turn the valve off by making the voltage
LOW
delay(30000);                 // reaction time
digitalWrite(Valve_Vent, HIGH);   // turn the valve on (HIGH is the voltage
level)
delay(1000);                 // wait for a second
digitalWrite(Valve_Vent, LOW);    // turn the valve off by making the voltage
LOW
delay(3000);                 // reaction time
digitalWrite(Valve_Feed, HIGH);   // turn the valve on (HIGH is the voltage
level)
delay(1500);                 // wait for a second
digitalWrite(Valve_Feed, LOW);    // turn the valve off by making the voltage
LOW
delay(30000);                 // reaction time
digitalWrite(Valve_Vent, HIGH);   // turn the valve on (HIGH is the voltage
level)
delay(1000);                 // wait for a second
digitalWrite(Valve_Vent, LOW);    // turn the valve off by making the voltage
LOW
delay(3000);                 // reaction time
digitalWrite(Valve_Feed, HIGH);   // turn the valve on (HIGH is the voltage
level)
delay(1500);                 // wait for a second
digitalWrite(Valve_Feed, LOW);    // turn the valve off by making the voltage
LOW
delay(30000);                 // reaction time
```

```
digitalWrite(Valve_Vent, HIGH);   // turn the valve on (HIGH is the voltage
level)
delay(1000);                // wait for a second
digitalWrite(Valve_Vent, LOW);    // turn the valve off by making the voltage
LOW
delay(3000);                // reaction time
digitalWrite(Valve_Feed, HIGH);   // turn the valve on (HIGH is the voltage
level)
delay(1500);                // wait for a second
digitalWrite(Valve_Feed, LOW);    // turn the valve off by making the voltage
LOW
delay(30000);                // reaction time
digitalWrite(Valve_Vent, HIGH);   // turn the valve on (HIGH is the voltage
level)
delay(1000);                // wait for a second
digitalWrite(Valve_Vent, LOW);    // turn the valve off by making the voltage
LOW
delay(3000);                // reaction time
digitalWrite(Valve_Feed, HIGH);   // turn the valve on (HIGH is the voltage
level)
delay(1500);                // wait for a second
digitalWrite(Valve_Feed, LOW);    // turn the valve off by making the voltage
LOW
delay(30000);                // reaction time
digitalWrite(Valve_Vent, HIGH);   // turn the valve on (HIGH is the voltage
level)
delay(1000);                // wait for a second
digitalWrite(Valve_Vent, LOW);    // turn the valve off by making the voltage
LOW
delay(3000);                // reaction time
digitalWrite(Valve_Feed, HIGH);   // turn the valve on (HIGH is the voltage
level)
delay(1500);                // wait for a second
digitalWrite(Valve_Feed, LOW);    // turn the valve off by making the voltage
LOW
delay(30000);                // reaction time
digitalWrite(Valve_Vent, HIGH);   // turn the valve on (HIGH is the voltage
level)
delay(1000);                // wait for a second
digitalWrite(Valve_Vent, LOW);    // turn the valve off by making the voltage
LOW
delay(3000);                // reaction time
digitalWrite(Valve_Feed, HIGH);   // turn the valve on (HIGH is the voltage
level)
delay(1500);                // wait for a second
digitalWrite(Valve_Feed, LOW);    // turn the valve off by making the voltage
LOW
delay(30000);                // reaction time
digitalWrite(Valve_Vent, HIGH);   // turn the valve on (HIGH is the voltage
level)
delay(1000);                // wait for a second
digitalWrite(Valve_Vent, LOW);    // turn the valve off by making the voltage
LOW
delay(3000);                // reaction time
digitalWrite(Valve_Feed, HIGH);   // turn the valve on (HIGH is the voltage
level)
delay(1500);                // wait for a second
```

```
digitalWrite(Valve_Feed, LOW);    // turn the valve off by making the voltage
LOW
delay(30000);               // reaction time
digitalWrite(Valve_Vent, HIGH);   // turn the valve on (HIGH is the voltage
level)
delay(1000);               // wait for a second
digitalWrite(Valve_Vent, LOW);    // turn the valve off by making the voltage
LOW
delay(3000);               // reaction time
digitalWrite(Valve_Feed, HIGH);   // turn the valve on (HIGH is the voltage
level)
delay(1500);               // wait for a second
digitalWrite(Valve_Feed, LOW);    // turn the valve off by making the voltage
LOW
delay(30000);               // reaction time
digitalWrite(Valve_Vent, HIGH);   // turn the valve on (HIGH is the voltage
level)
delay(1000);               // wait for a second
digitalWrite(Valve_Vent, LOW);    // turn the valve off by making the voltage
LOW
delay(3000);               // reaction time
digitalWrite(Valve_Feed, HIGH);   // turn the valve on (HIGH is the voltage
level)
delay(1500);               // wait for a second
digitalWrite(Valve_Feed, LOW);    // turn the valve off by making the voltage
LOW
delay(30000);               // reaction time
digitalWrite(Valve_Vent, HIGH);   // turn the valve on (HIGH is the voltage
level)
delay(1000);               // wait for a second
digitalWrite(Valve_Vent, LOW);    // turn the valve off by making the voltage
LOW
delay(3000);               // reaction time
digitalWrite(Valve_Feed, HIGH);   // turn the valve on (HIGH is the voltage
level)
delay(1500);               // wait for a second
digitalWrite(Valve_Feed, LOW);    // turn the valve off by making the voltage
LOW
delay(30000);               // reaction time
digitalWrite(Valve_Vent, HIGH);   // turn the valve on (HIGH is the voltage
level)
delay(1000);               // wait for a second
digitalWrite(Valve_Vent, LOW);    // turn the valve off by making the voltage
LOW
delay(3000);               // reaction time
digitalWrite(Valve_Feed, HIGH);   // turn the valve on (HIGH is the voltage
level)
delay(1500);               // wait for a second
digitalWrite(Valve_Feed, LOW);    // turn the valve off by making the voltage
LOW
delay(30000);               // reaction time
digitalWrite(Valve_Vent, HIGH);   // turn the valve on (HIGH is the voltage
level)
delay(1000);               // wait for a second
digitalWrite(Valve_Vent, LOW);    // turn the valve off by making the voltage
LOW
delay(3000);               // reaction time
```

```
digitalWrite(Valve_Feed, HIGH);   // turn the valve on (HIGH is the voltage
level)
delay(1500);                 // wait for a second
digitalWrite(Valve_Feed, LOW);    // turn the valve off by making the voltage
LOW
delay(30000);                 // reaction time
digitalWrite(Valve_Vent, HIGH);   // turn the valve on (HIGH is the voltage
level)
delay(1000);                 // wait for a second
digitalWrite(Valve_Vent, LOW);    // turn the valve off by making the voltage
LOW
delay(3000);                 // reaction time
digitalWrite(Valve_Feed, HIGH);   // turn the valve on (HIGH is the voltage
level)
delay(1500);                 // wait for a second
digitalWrite(Valve_Feed, LOW);    // turn the valve off by making the voltage
LOW
delay(30000);                 // reaction time
digitalWrite(Valve_Vent, HIGH);   // turn the valve on (HIGH is the voltage
level)
delay(1000);                 // wait for a second
digitalWrite(Valve_Vent, LOW);    // turn the valve off by making the voltage
LOW}
// the loop routine runs over and over again forever:
void loop() {}
```

Appendix C Calibration

C.1 GC Details

A gas chromatograph (Agilent 7890B), shown in Figure C.1, was used to measure the molar concentration of the gas phase products. The GC has three channels, two thermal conductivity detectors (TCD) and one flame ionization detector (FID). The first TCD channel uses hydrogen as a carrier gas to measure the concentration of oxygen, nitrogen, carbon dioxide, and carbon monoxide. The second TCD channel uses argon as a carrier gas to measure the concentration of helium and hydrogen. The TCD channels measure the concentration of the sample by comparing the thermal conductivity of two flows, one with just the carrier gas and the other with the carrier gas and the sample. The difference in thermal conductivity determines which species and the molar concentration of the species with the carrier gas. Argon had to be used as a carrier gas instead of hydrogen in one of the TCD channels to measure the concentration of hydrogen. The detector temperature was 200 °C for both TCD channels and the carrier gas had a flow rate of 45 mL/min. The FID channel uses hydrogen as a carrier gas, nitrogen as a make-up gas, and air to ignite the hydrogen to measure the concentration of methane, ethane, ethylene, propane, acetylene, and benzene for this method. The FID channel measures the concentration of the sample by burning the sample mixed with the carrier gas with a hydrogen-air flame that burns the organic components to create ions. These ions are then collected and tested to determine the concentration of the hydrocarbons. The detector temperature was 523 K for the FID channel and hydrogen, air, and nitrogen had flowrates of 40 mL/min, 400 ml/min, and 25 mL/min, respectively. Table C.1 shows the columns that are used in the GC to separate the components in the sample before sending them to the detectors to be analyzed.

Figure C.1: Agilent 7890B GC. (Figure taken from Agilent 2021).

Table C.1: Columns used in GC (as seen in Falahati 2018)

Column number	Length (m)	Diameter (mm)	Model Number
1	60	0.25	CP8780
2	0.5	2	G3591-81023
3	1.83	2	G3591-81037
4	2.44	2	G3591-80022
5	0.91	2	G3591-81135
6	1.83	2	G3591-81035

C.2 Procedure for Calibrating

This standard operating procedure outlines a typical step by step procedure of calibrating and analyzing a gas sample with a gas chromatography device for data used in this experiment. As the exact testing procedure may change for other experiments due to different in gas sampling methods. Table C.2 shows the gas concentrations for all the gases used to calibrate the GC.

1. Check carrier gas cylinders to make sure they are not empty (hydrogen, air, argon, and nitrogen). If they are close to being empty order a new cylinder.
2. Check that the valve on the building air supply that connects to the GC is open and pressure is set at 40psi.
3. Run “Furnace Pyrolysis Method” on the GC online software and wait until the GC gives the green “Ready” sign on the screen.
4. Choose run method and put in a name and details of the standard used for this calibration.
5. Wait for purple “Waiting for Injection” sign on the software.
6. Connect the outlet of the GC to a manual pressure gauge and to a line that goes to the fume hood and make sure all connections and the tubing are in a good condition.
7. Connect the inlet of the GC to the standard cylinder and ensure that the correct fitting is on the regulator and all the connection are sealed.
8. If the standard contains CO setup two CO monitors and place one by the cylinder and one by where you are working.
9. Open the pressure valve on the regulator all the way counterclockwise (to ensure the pressure would be zero if you were to open the valve on the cylinder).
10. Slowly open the valve on the cylinder and the outlet valve on the regulator.

11. Now slowly turn the pressure valve on the regulator and set the pressure between 5-10psi. Check the flow by placing the outlet tube, that is in the fume hood, in a water container and bubbles are created. Take the tube out of the container and keep it in the fume hood and fix it so it does not move.
12. Let the standard purge for around 10 minutes then close the valve on both the cylinder and regulator.
13. Wait and track the pressure inside the GC until the gauge reads 0psi.
14. Hit the start button on the GC and wait 20 minutes for method to complete.
15. After the method is done compare the results with the certification on the standard, if the results are in an acceptable range; choose calibration -> recalibration-> put the right level number -> select replace and press OK.
16. If running the standard for the first time choose Calibration -> Add level -> Put level number -> Ok-> Calibration -> Add peak -> choose the same level number -> and in the calibration table while it is set on “Peak Details” put the name and actual concentration for new components and press OK.
17. After calibrating and recalibrating all desired standards, save the method.
18. Make sure the valve on the standard is closed. Disconnect the regulator from the standard and put the cap on the bottle return the bottle to a secured spot.
19. Put the GC back to “Standby Method”.
20. Clean up the experimental bench.

Table C.2: Calibration data for gas chromatograph

Standard #	Gas Molar Concentration (%)												
	H_2	He	N_2	O_2	CO	CO_2	CH_4	C_2H_2	C_2H_4	C_2H_6	C_3H_8	C_4H_{10}	C_6H_6
	Hydrogen	Helium	Nitrogen	Oxygen	Carbon monoxide	Carbon dioxide	Methane	Acetylene	Ethylene	Ethane	Propane	Butane	Benzene
1			93.88	1.01	0.0998	5.01							
2	0.4018		79.449		19.95		0.1002			0.09975	0.09937		
3			99.889	0.1005	0.01								
5	4.005		92.979				0.9947			1.013	1.008		
6	19.93		65.035				4.971			4.994	5.07		
9			57.055	19.99	3.005	19.95							
10			85.396	3.992	0.6016	10.01							
11	0.04		89.946		9.983		0.0105			0.0101	0.0102		
12			1.76			0.8108	94.96			2.4	0.0589	0.0103	
13		0.02	49.9			0.01	49.97					0.1	
14		0.1006	99.79971			0.09969							
15		0.05	99.905802			0.0402	0.001			0.001	0.001	0.001	
16			99.695					0.102	0.102				0.101
17			99.98468					0.00512	0.00508				0.00512
18	50.44						49.56						
19		0.1					99.9						

C.2 Calibration Results

Table C.3 shows the retention times, area, response factor, standard number, and the mole fraction for each of the calibration gases used. Figure C.2 – Figure C.12 show the calibration results for each species. Table C.4 shows the relative differences for all measured species.

Table C.3: GC calibration data

Compound	Time window (min)	Retention Time (min)	Standard #	Molar Concentration (%)	Area	Response Factor
Helium	0.610 - 0.709	0.657	13	0.02	30.98	6.45575×10^{-4}
			15	0.05	75.15	6.65362×10^{-4}
			19	0.10	151.79	6.58810×10^{-4}
			14	0.1006	152.81	6.58330×10^{-4}
Hydrogen	0.710 - 1.050	0.788	5	4.005	10129.00	3.95443×10^{-4}
			6	19.93	50538.20	3.94355×10^{-4}
			18	50.44	127412.00	3.95880×10^{-4}
Methane	1.106 - 1.264	1.144	15	0.001	2.29	4.36698×10^{-4}
			5	0.9947	2209.10	4.50275×10^{-4}
			6	4.971	11658.80	4.26373×10^{-4}
			18	49.56	114784.00	4.31768×10^{-4}
			13	49.97	115522.00	4.32559×10^{-4}
			12	94.96	216317.00	4.38985×10^{-4}
			19	99.9	226873.00	4.40334×10^{-4}
Ethane	1.308- 1.602	1.42	15	0.001	4.29	2.33053×10^{-4}
			5	1.013	4251.83	2.38251×10^{-4}
			12	2.4	10843.90	2.21323×10^{-4}
			6	4.994	22304.40	2.23902×10^{-4}
Ethylene	1.830 - 1.985	1.937	17	0.00508	22.82	2.22572×10^{-4}
			16	0.102	432.80	2.35677×10^{-4}
Propane	2.697 - 3.147	2.959	15	0.001	6.54	1.52889×10^{-4}
			12	0.0589	404.78	1.45511×10^{-4}
			5	1.008	6387.74	1.57802×10^{-4}
			6	5.07	33730.10	1.50311×10^{-4}
CO2	3.270 - 4.070	3.67	12	0.8108	1431.28	5.66486×10^{-4}
			1	5.01	9008.28	5.56155×10^{-4}
			10	10.01	18321.90	5.46340×10^{-4}
			9	19.95	37438.60	5.32873×10^{-4}

Compound	Time window (min)	Retention Time (min)	Standard #	Molar Concentration (%)	Area	Response Factor
O2	5.548 - 5.833	5.653	3	0.1005	178.96	5.61585×10^{-4}
			1	1.01	1617.02	6.24607×10^{-4}
			10	3.992	6746.77	5.91691×10^{-4}
			9	19.99	33911.50	5.89476×10^{-4}
Nitrogen	5.904 - 6.488	6.065	12	1.76	3506.68	5.01900×10^{-4}
			13	49.9	95689.80	5.21477×10^{-4}
			6	65.035	121861.00	5.33683×10^{-4}
			10	85.396	158727.00	5.38005×10^{-4}
			5	92.979	172454.00	5.39151×10^{-4}
			15	99.906	186462.00	5.35797×10^{-4}
			17	99.98468	185418.00	5.39239×10^{-4}
Acetylene	6.820 - 8.392	7.336	17	0.00512	24.88	2.05748×10^{-4}
			16	0.102	554.22	1.84043×10^{-4}
CO	7.610 - 9.110	8.11	1	0.0998	196.21	5.08651×10^{-4}
			10	0.6016	1178.73	5.10380×10^{-4}
			9	3.005	5964.02	5.03855×10^{-4}
			11	9.983	19404.60	5.14467×10^{-4}
			2	19.95	38356.80	5.20117×10^{-4}
Benzene	16.905-18.106	17.406	17	0.00512	68.28	7.49817×10^{-5}
			16	0.101	1270.77	7.94797×10^{-5}

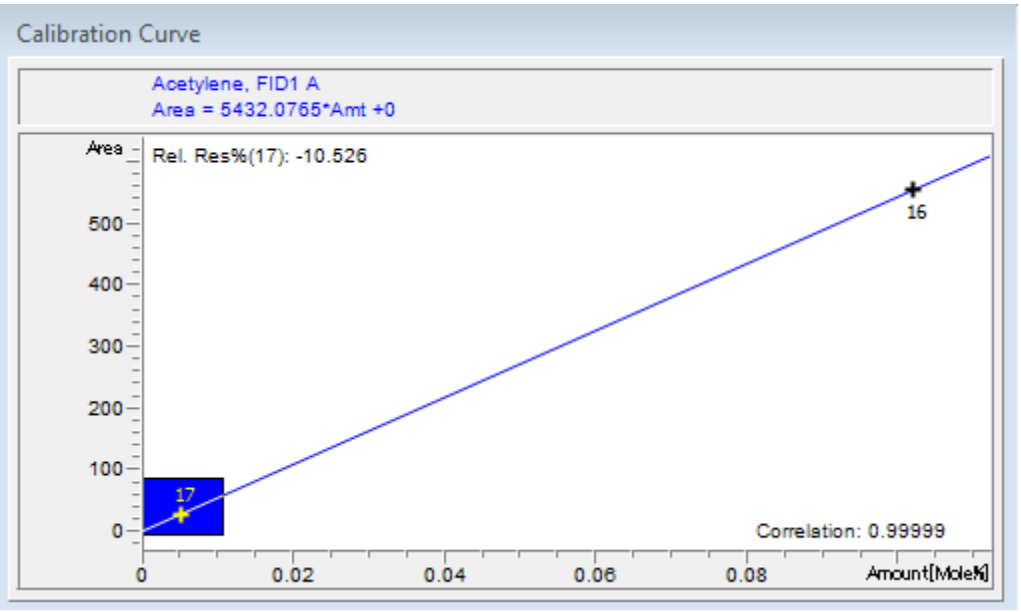

Figure C.2: Acetylene calibration curve

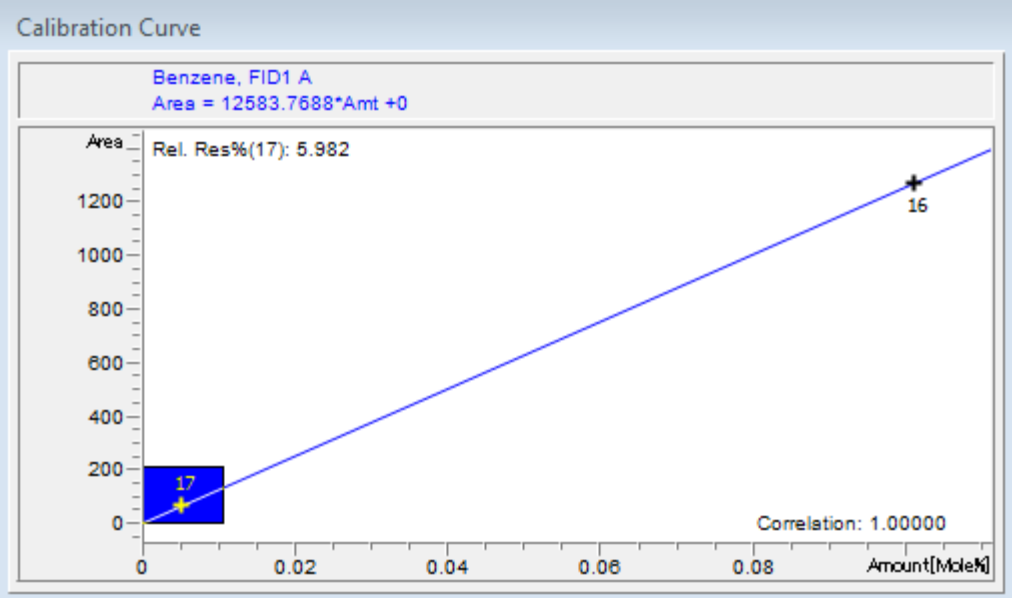

Figure C.3: Benzene calibration curve

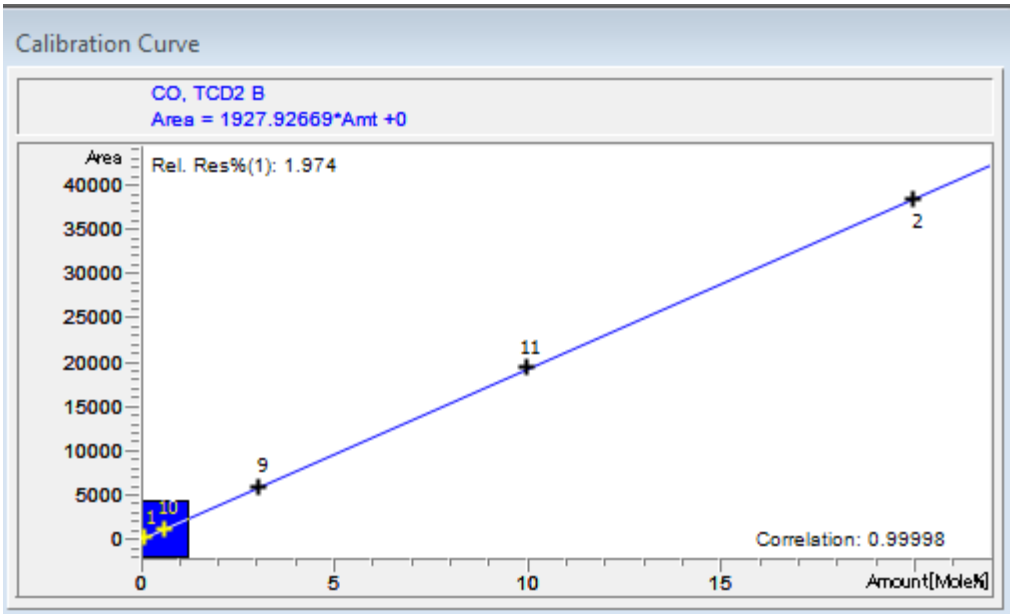

Figure C.4: Carbon monoxide calibration curve

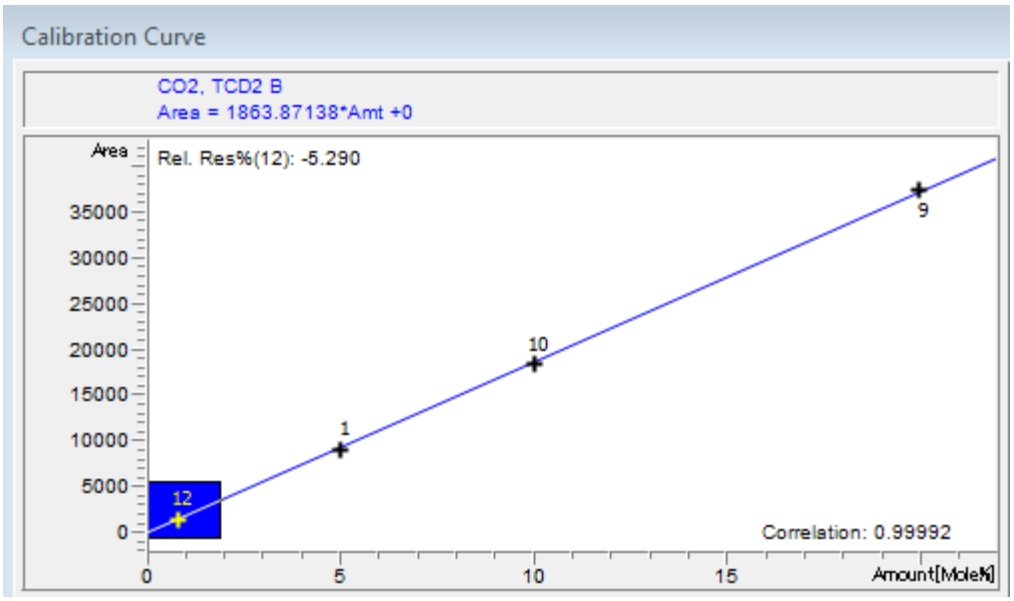

Figure C.5: Carbon dioxide calibration curve

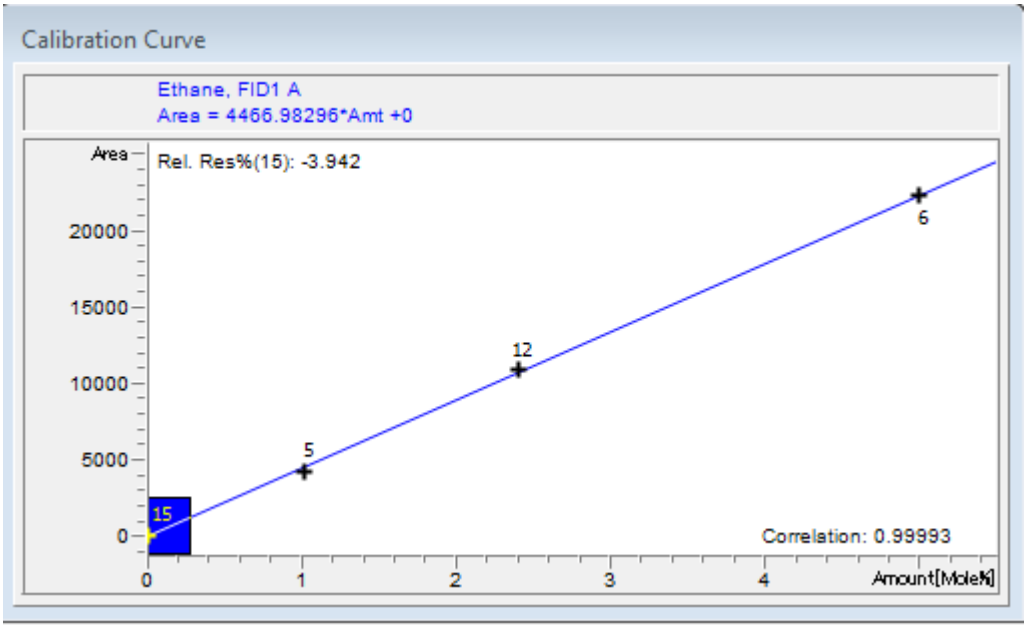

Figure C.6: Ethane calibration curve

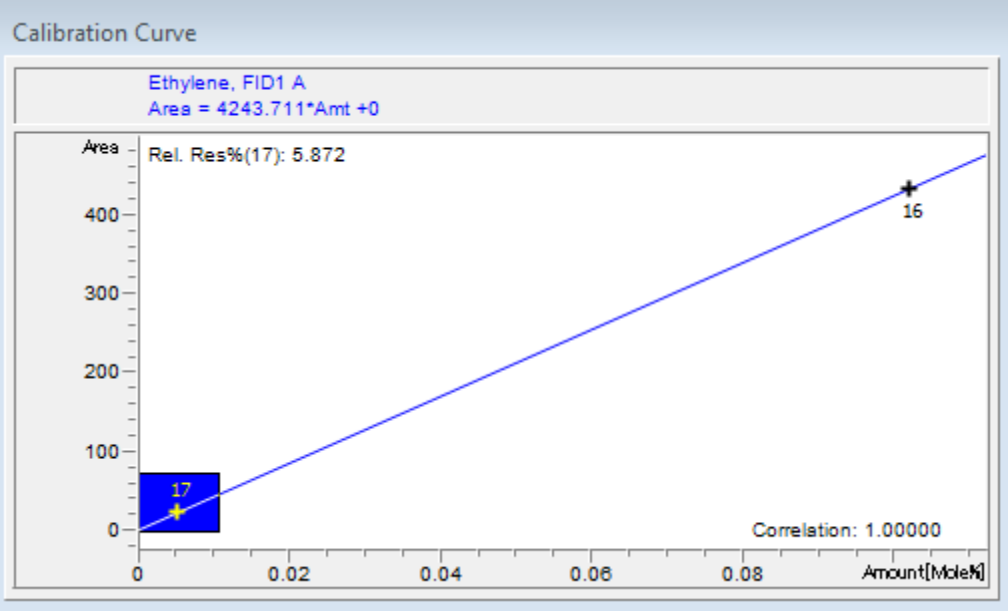

Figure C.7: Ethylene calibration curve

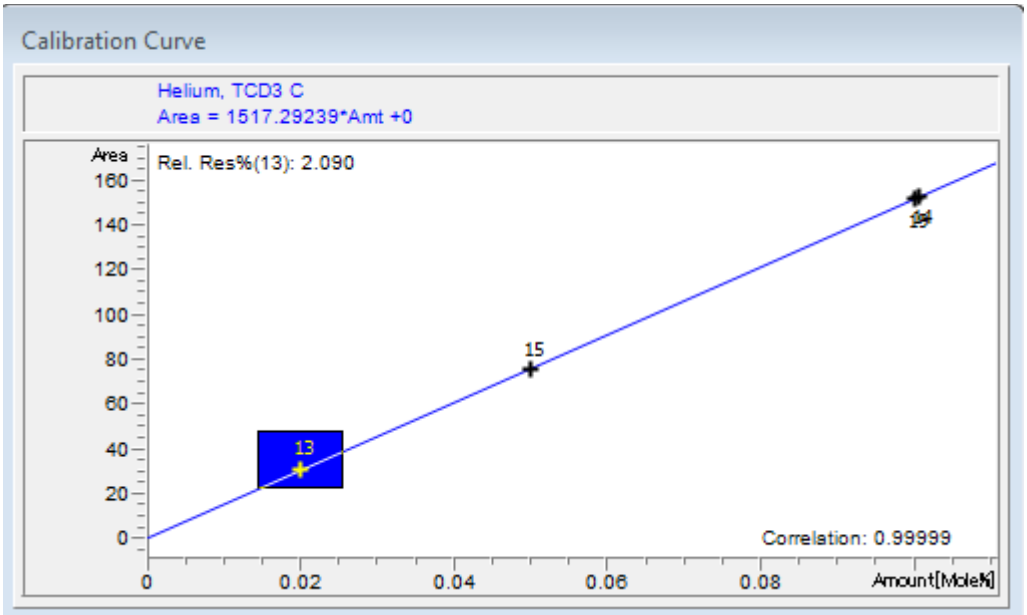

Figure C.8: Helium calibration curve

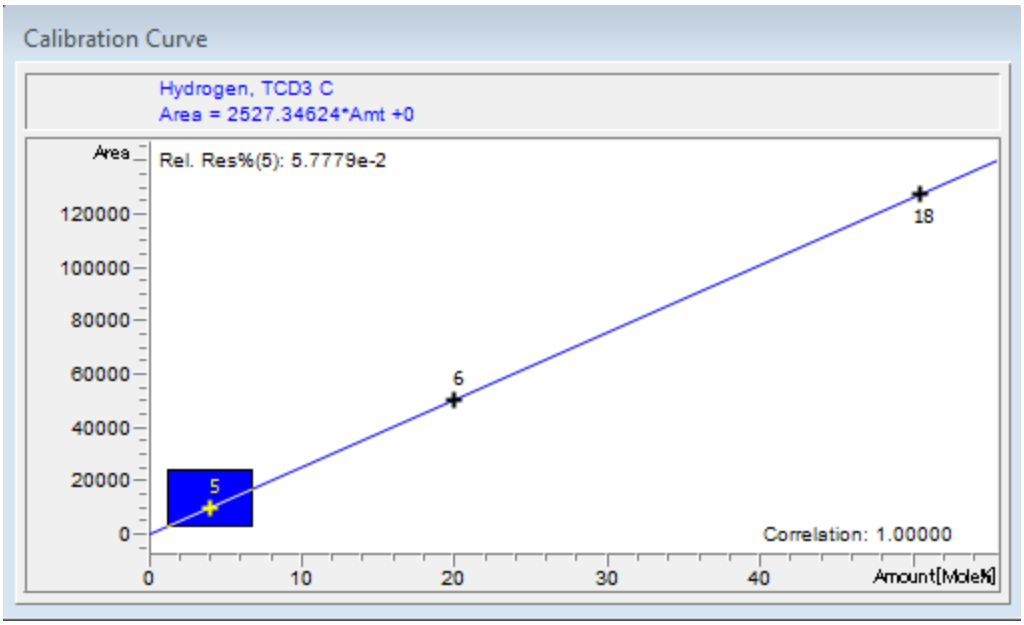

Figure C.9: Hydrogen calibration curve

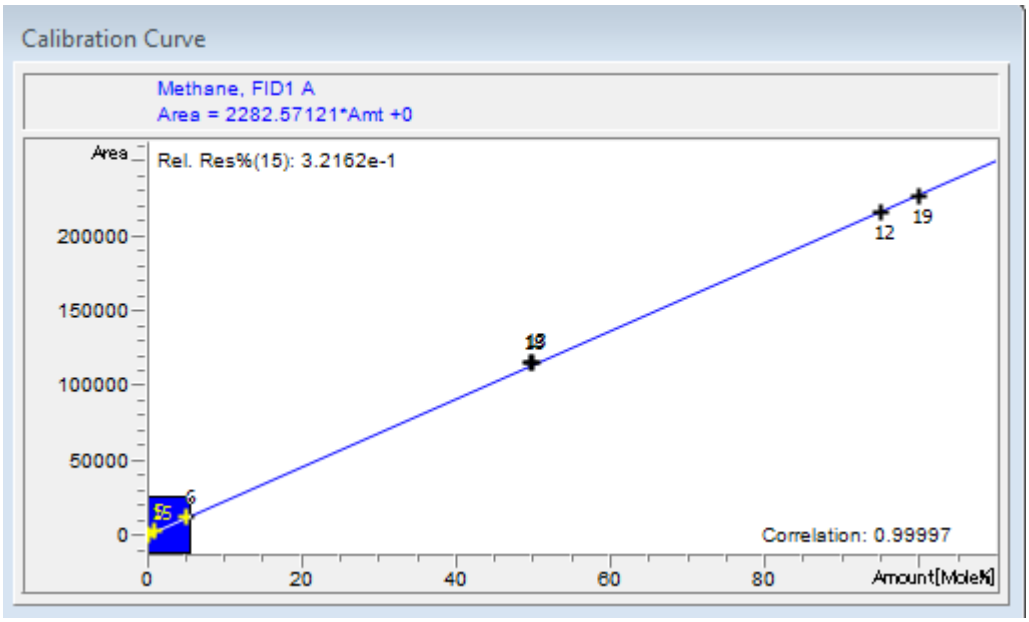

Figure C.10: Methane calibration curve

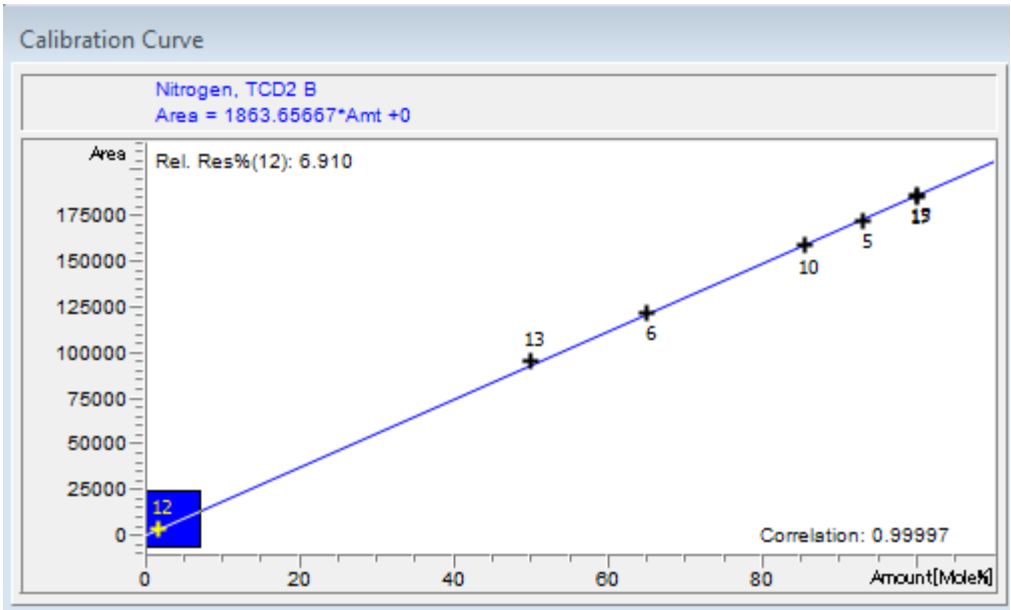

Figure C.11: Nitrogen calibration curve

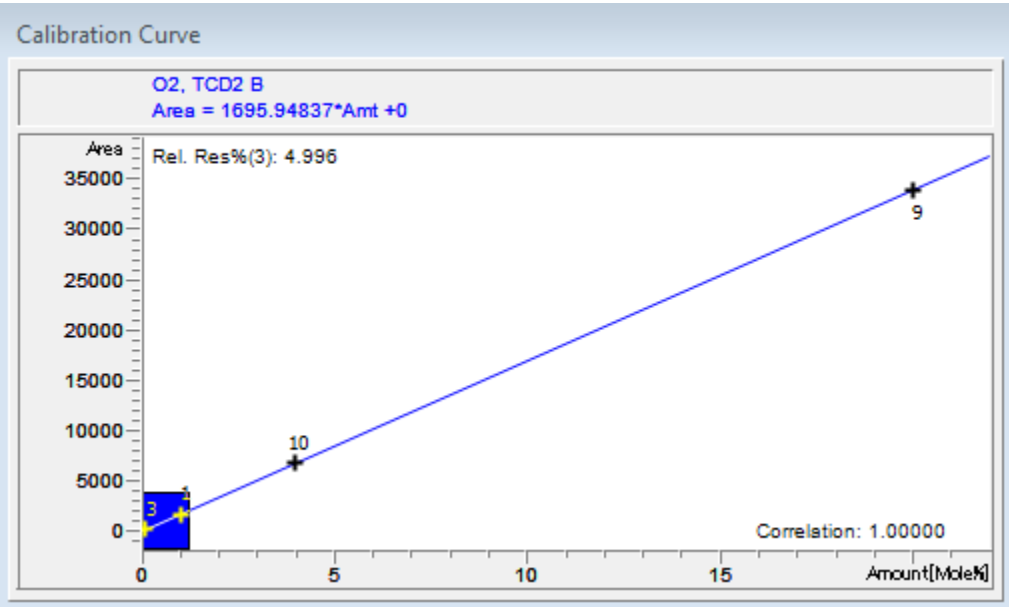

Figure : Oxygen calibration curve

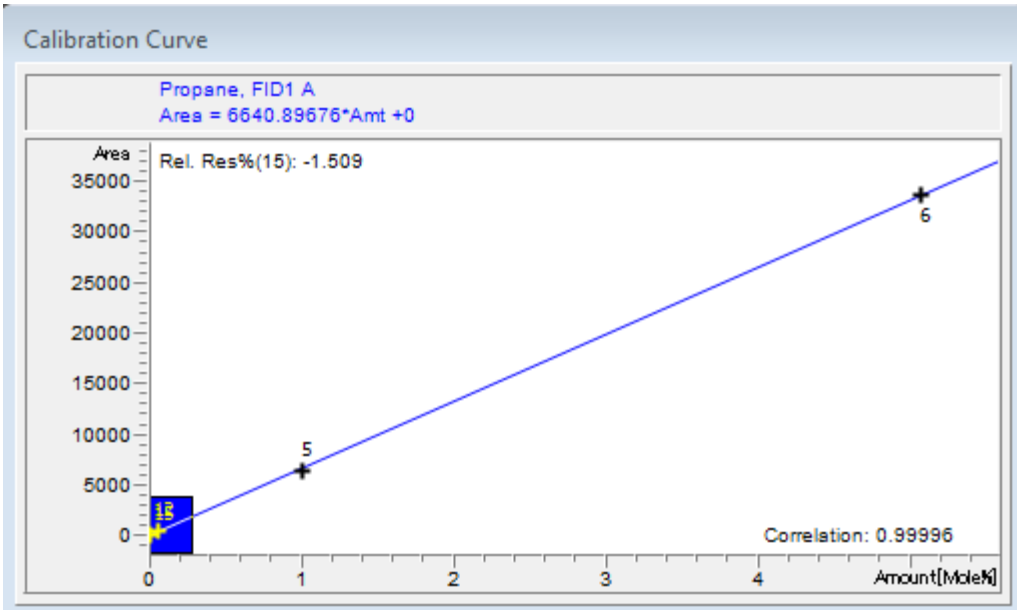

Figure C.12: Propane calibration curve

Table C.4: GC relative differences for all measured species (E is the maximum relative difference).

Compound	Standard #	Number of tests	Standard Molar Concentration (%)	Area	Equation from calibration curve	Measured Concentration (%)	Relative Difference	E
Helium	13	5	0.02	30.98	1517.29	0.02042	0.020902	0.0209
	15	4	0.05	75.15	1517.29	0.04953	0.009459	
	19	6	0.10	151.79	1517.29	0.10004	0.000393	
	14	3	0.1006	152.81	1517.29	0.10071	0.001122	
Hydrogen	5	5	4.005	10129.00	2527.35	4.00776	0.000689	0.0033
	6	5	19.93	50538.20	2527.35	19.99655	0.003339	
	18	5	50.44	127412.00	2527.35	50.41335	0.000528	
Methane	15	4	0.001	2.29	2282.57	0.00100	0.003215	0.0275
	5	5	0.9947	2209.10	2282.57	0.96781	0.027033	
	6	5	4.971	11658.80	2282.57	5.10775	0.027509	
	18	5	49.56	114784.00	2282.57	50.28715	0.014672	
	13	5	49.97	115522.00	2282.57	50.61047	0.012817	
	12	5	94.96	216317.00	2282.57	94.76900	0.002011	
	19	6	99.9	226873.00	2282.57	99.39361	0.005069	
Ethane	15	4	0.001	4.29	4466.98	0.00096	0.039423	0.0604
	5	5	1.013	4251.83	4466.98	0.95183	0.060381	
	12	5	2.4	10843.90	4466.98	2.42757	0.011486	
	6	5	4.994	22304.40	4466.98	4.99317	0.000166	
Ethylene	17	3	0.00508	22.82	4243.71	0.00538	0.058725	0.0587
	16	3	0.102	432.80	4243.71	0.10199	0.000146	
Propane	15	4	0.001	6.54	6640.90	0.00098	0.015091	0.0458
	12	5	0.0589	404.78	6640.90	0.06095	0.034852	
	5	5	1.008	6387.74	6640.90	0.96188	0.045755	
	6	5	5.07	33730.10	6640.90	5.07915	0.001804	

Compound	Standard #	Number of tests	Standard Molar Concentration (%)	Area	Equation from calibration curve	Measured Concentration (%)	Relative Difference	E
CO2	12	5	0.8108	1431.28	1863.87	0.76791	0.052902	0.0529
	1	4	5.01	9008.28	1863.87	4.83310	0.035309	
	10	4	10.01	18321.90	1863.87	9.83002	0.017980	
	9	4	19.95	37438.60	1863.87	20.08647	0.006841	
O2	3	4	0.1005	178.96	1695.95	0.10552	0.049958	0.0560
	1	4	1.01	1617.02	1695.95	0.95346	0.055981	
	10	4	3.992	6746.77	1695.95	3.97817	0.003465	
	9	4	19.99	33911.50	1695.95	19.99560	0.000280	
Nitrogen	12	5	1.76	3506.68	1863.66	1.88161	0.069097	0.0691
	13	5	49.9	95689.80	1863.66	51.34519	0.028962	
	6	5	65.035	121861.00	1863.66	65.38812	0.005430	
	10	4	85.396	158727.00	1863.66	85.16966	0.002651	
	5	5	92.979	172454.00	1863.66	92.53528	0.004772	
	15	4	99.906	186462.00	1863.66	100.05169	0.001458	
	17	3	99.98468	185418.00	1863.66	99.49150	0.004933	
Acetylene	17	3	0.00512	24.88	5432.08	0.00458	0.105258	0.1053
	16	3	0.102	554.22	5432.08	0.10203	0.000265	
CO	1	4	0.0998	196.21	1927.93	0.10177	0.019740	0.0294
	10	4	0.6016	1178.73	1927.93	0.61140	0.016286	
	9	4	3.005	5964.02	1927.93	3.09349	0.029448	
	11	4	9.983	19404.60	1927.93	10.06501	0.008215	
	2	5	19.95	38356.80	1927.93	19.89536	0.002739	
Benzene	17	3	0.00512	68.28	12583.77	0.00543	0.059825	0.0598
	16	3	0.101	1270.77	12583.77	0.10098	0.000154	

Appendix D Daily Check on Calibration

Figure D.1 shows the results of running a calibration gas through the GC every day before running experiments. Methane was found to have a mole fraction of 49.88 ± 1.39 and hydrogen was found to have a mole fraction of 50.02 ± 0.21. The expected values were 49.56 and 50.44 for methane and hydrogen, respectively. This is a relative uncertainty of 0.64% and 0.83% for methane and hydrogen, respectively. The uncertainty is mostly due to the bias uncertainty of the GC and therefore within the accepted uncertainty without the GC needing to be recalibrated. Table D.1 shows the molar concentrations from the daily checks used to make Figure D.1.

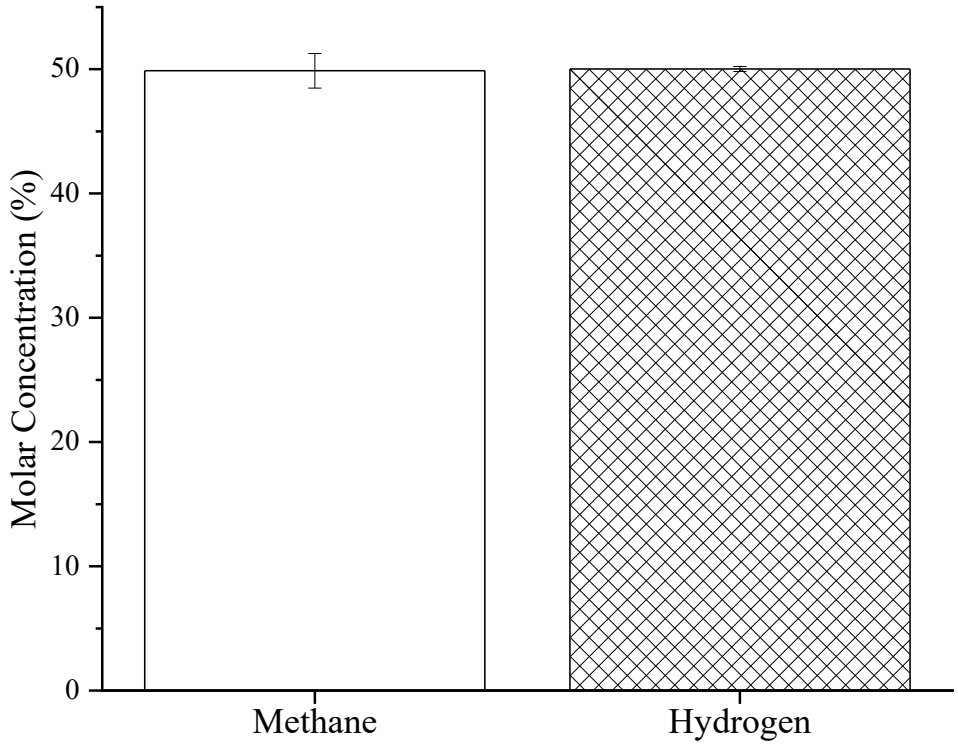

Figure D.1: Daily check uncertainty.

Table D.1: Daily check on calibration data.

Date	Molar Concentration (%)		
	Methane	Hydrogen	Sum
11-Feb	48.4	50.8	99.2
17-Feb	48.2	50.2	98.3
01-Mar	49.8	49.6	99.4
02-Mar	49.7	49.7	99.4
03-Mar	49.9	49.7	99.6
04-Mar	50.1	50.0	100.1
05-Mar	49.9	50.0	99.9
06-Mar	49.7	49.8	99.5
08-Mar	50.1	50.2	100.2
09-Mar	50.0	50.0	99.9
10-Mar	50.2	50.3	100.5
15-Mar	50.1	50.1	100.2
23-Mar	50.4	50.2	100.6
23-Mar	50.5	50.1	100.6
24-Mar	49.8	49.6	99.3
25-Mar	50.0	49.9	99.9
26-Mar	50.0	49.9	99.9
30-Mar	50.2	50.2	100.4
31-Mar	50.1	50.1	100.2
01-Apr	49.8	49.4	99.2
13-Apr	50.7	50.6	101.4

Appendix E Experimental Results

The results for the completed experiments can be found in Table E.1 – Table E.9. Table E.1 – Table E.3 shows the results for experiments completed with the oven temperature at 873 K with an initial pressure of 399 kPa. Table E.4 – Table E.6 shows the results for experiments completed with the oven temperature at 1073 K with an initial pressure of 399 kPa. Table E.7 – Table E.9 shows the results for experiments completed with the oven temperature at 1273 K with an initial pressure of 399 kPa.

Table E.10 shows the average final pressure and its uncertainty for the experiments completed.

Table E.1: Results for hydrocarbons and hydrogen with an oven temperature setpoint of 873 K and an initial pressure of 399 kPa.

Reaction time (s)	Temperature (K)	Final Pressure (kPa)	Molar Concentration (%)						
			Methane	Ethane	Ethylene	Propane	Acetylene	Benzene	Hydrogen
15	895	435	77.27	0.0067	0.00028	ND	ND	ND	16.00
15	894	424	83.98	0.0439	0.00200	ND	ND	ND	9.45
15	900	413	94.14	0.0059	ND	ND	ND	ND	4.60
15	896	440	81.83	0.0052	0.00025	ND	ND	ND	15.39
15	899	413	90.83	0.1686	0.07461	0.00335	ND	ND	3.13
30	886	443	77.05	0.0095	0.00034	ND	ND	ND	17.01
30	890	440	78.63	0.0381	0.00087	ND	ND	ND	15.25
30	887	439	78.09	0.0590	0.00176	0.00059	ND	0.00220	14.92
30	897	452	77.87	0.0050	ND	ND	ND	ND	20.28
60	887	450	74.57	0.0299	0.00337	ND	ND	ND	18.20
60	886	448	75.93	0.0338	0.00412	ND	ND	0.00221	17.56
60	893	456	72.32	0.0052	0.00059	ND	ND	0.00238	21.71
180	900	469	68.70	0.0110	0.00277	ND	ND	ND	24.60
180	887	464	69.88	0.0105	0.00284	ND	ND	ND	23.35
180	887	465	69.80	0.0052	0.00034	ND	ND	ND	23.88
180	886	464	70.55	0.0065	0.00056	ND	ND	ND	23.27
180	889	465	69.39	0.0057	0.00040	ND	ND	ND	24.11
300	894	467	71.51	0.0066	0.00081	ND	ND	ND	25.06
300	893	468	71.72	0.0054	0.00044	ND	ND	0.00036	25.35
300	893	470	70.80	0.0041	0.00024	ND	ND	ND	26.09
300	889	473	67.53	0.0103	0.00338	ND	ND	0.00228	26.32
300	886	467	67.96	0.0089	0.00277	ND	ND	0.00360	25.92

ND = not detected

Table E.2: Results for other measured species in the products with an oven temperature setpoint of 873 K and an initial pressure of 399 kPa.

Reaction time (s)	Temperature (K)	Final Pressure (kPa)	Molar Concentration (%)						Scaling factor*
			CO2	O2	Nitrogen	CO	Helium	Sum	
15	895	435	0.296	0.570	4.04	ND	ND	99.31	1.049
15	894	424	0.504	0.533	3.93	ND	ND	99.31	1.050
15	900	413	0.099	0.138	0.77	ND	0.054	99.98	1.010
15	896	440	0.159	0.040	0.90	ND	0.040	99.20	1.011
15	899	413	ND	0.932	3.85	ND	ND	99.61	1.048
30	886	443	0.344	0.492	3.80	ND	ND	99.87	1.046
30	890	440	0.417	0.505	3.83	ND	ND	99.80	1.048
30	887	439	ND	0.556	4.13	ND	ND	99.43	1.047
30	897	452	ND	0.068	0.93	ND	0.058	99.21	1.010
60	887	450	0.396	0.535	4.03	ND	ND	99.15	1.050
60	886	448	0.380	0.448	3.60	ND	ND	99.29	1.045
60	893	456	0.254	0.439	3.45	ND	ND	99.34	1.042
180	900	469	0.261	0.499	3.93	ND	ND	99.20	1.047
180	887	464	0.290	0.508	3.91	ND	ND	99.08	1.048
180	887	465	0.282	0.473	3.69	ND	ND	99.15	1.045
180	886	464	0.296	0.479	3.61	ND	ND	99.27	1.044
180	889	465	0.286	0.514	3.73	ND	ND	99.10	1.046
300	894	467	0.088	0.155	1.72	ND	0.037	99.16	1.020
300	893	468	0.072	0.088	1.28	ND	0.027	99.04	1.015
300	893	470	0.082	0.112	1.39	ND	0.021	98.98	1.016
300	889	473	0.313	0.470	3.70	ND	ND	99.40	1.045
300	886	467	0.317	0.445	3.60	ND	ND	99.27	1.044

*Scaling factor is used for normalizing the data.
ND = not detected

Table E.3: Normalized results for hydrocarbons, helium, and hydrogen with an oven temperature setpoint of 873 K and an initial pressure of 399 kPa.

Reaction time (s)	Temperature (K)	Final Pressure (kPa)	Molar Concentration (%)							
			Methane	Ethane	Ethylene	Propane	Acetylene	Benzene	Helium	Hydrogen
15	895	435	81.09	0.0070	0.00029	ND	ND	ND	ND	16.79
15	894	424	88.18	0.0461	0.00210	ND	ND	ND	ND	9.92
15	900	413	95.09	0.0060	ND	ND	ND	ND	0.05	4.65
15	896	440	82.74	0.0053	0.00026	ND	ND	ND	0.04	15.56
15	899	413	95.20	0.1767	0.07819	0.00351	ND	ND	ND	3.28
30	886	443	80.63	0.0100	0.00036	ND	ND	ND	ND	17.80
30	890	440	82.37	0.0399	0.00091	ND	ND	ND	ND	15.97
30	887	439	81.77	0.0617	0.00184	0.00062	ND	0.00230	ND	15.62
30	897	452	78.65	0.0051	ND	ND	ND	ND	0.06	20.48
60	887	450	78.30	0.0314	0.00354	ND	ND	ND	ND	19.11
60	886	448	79.32	0.0353	0.00430	ND	ND	0.00231	ND	18.34
60	893	456	75.34	0.0054	0.00061	ND	ND	0.00248	ND	22.61
180	900	469	71.94	0.0115	0.00291	ND	ND	ND	ND	25.76
180	887	464	73.20	0.0110	0.00297	ND	ND	ND	ND	24.46
180	887	465	72.93	0.0054	0.00036	ND	ND	ND	ND	24.95
180	886	464	73.67	0.0068	0.00059	ND	ND	ND	ND	24.30
180	889	465	72.56	0.0060	0.00042	ND	ND	ND	ND	25.22
300	894	467	72.93	0.0067	0.00082	ND	ND	ND	0.04	25.56
300	893	468	72.77	0.0054	0.00045	ND	ND	0.00037	0.03	25.71
300	893	470	71.93	0.0042	0.00024	ND	ND	ND	0.02	26.51
300	889	473	70.58	0.0108	0.00353	ND	ND	0.00238	ND	27.51
300	886	467	70.94	0.0093	0.00289	ND	ND	0.00376	ND	27.06

ND = not detected

Table E.4: Results for hydrocarbons and hydrogen with an oven temperature setpoint of 1073 K and an initial pressure of 399 kPa.

Reaction time (s)	Temperature (K)	Final Pressure (kPa)	Molar Concentration (%)						
			Methane	Ethane	Ethylene	Propane	Acetylene	Benzene	Hydrogen
15	1095	417	77.82	0.00312	0.00144	ND	ND	0.00060	14.79
15	1093	425	74.75	0.00355	0.00107	ND	ND	ND	16.82
15	1091	424	75.15	0.00369	0.00098	ND	ND	ND	16.64
15	1094	431	71.86	0.00377	0.00070	ND	ND	ND	20.03
15	1089	443	65.24	0.00117	0.00045	ND	ND	ND	25.58
15	1088	442	65.53	0.00168	0.00046	ND	ND	ND	25.57
15	1088	443	64.75	0.00242	0.00044	ND	ND	ND	26.16
30	1093	430	80.19	0.00087	0.00087	ND	ND	ND	18.06
30	1090	441	73.67	0.00069	0.00062	ND	ND	ND	24.05
30	1092	432	78.78	0.00109	0.00087	ND	ND	ND	19.27
30	1091	468	57.10	0.00216	0.00043	ND	ND	ND	34.30
30	1092	466	57.55	0.00080	0.00044	ND	ND	ND	33.26
60	1098	495	54.97	0.00034	0.00042	ND	ND	ND	42.22
60	1096	446	76.05	0.00055	0.00093	ND	ND	ND	22.85
60	1095	454	72.09	0.00045	0.00072	ND	ND	ND	26.49
60	1094	449	74.31	0.00073	0.00083	ND	ND	ND	24.31
60	1095	492	49.95	0.00201	0.00044	ND	ND	ND	41.05
60	1095	490	50.32	0.00197	0.00044	ND	ND	ND	40.67
60	1094	492	50.35	0.00148	0.00043	ND	ND	ND	40.73
180	1095	519	42.05	0.00154	0.00039	ND	ND	ND	49.76
180	1096	518	42.63	0.00164	0.00041	ND	ND	ND	49.12
180	1096	518	42.56	0.00082	0.00041	ND	ND	ND	49.11
180	1096	519	42.60	0.00157	0.00039	ND	ND	ND	49.13
180	1086	520	46.61	0.00074	0.00046	ND	ND	ND	48.92
180	1086	518	46.00	ND	0.00042	ND	ND	ND	48.67
180	1086	526	44.69	0.00085	0.00038	ND	ND	ND	51.10

Reaction time (s)	Temperature (K)	Final Pressure (kPa)	Molar Concentration (%)						
			Methane	Ethane	Ethylene	Propane	Acetylene	Benzene	Hydrogen
180	1090	522	45.42	0.00084	0.00041	ND	ND	ND	50.63
180	1089	527	45.24	0.00092	0.00041	ND	ND	ND	51.55
180	1093	525	45.96	ND	0.00045	ND	ND	ND	50.88
300	1100	521	49.07	0.00071	0.00081	ND	ND	ND	47.71
300	1097	513	50.51	0.00218	0.00092	ND	ND	ND	46.09
300	1101	530	40.18	0.00244	0.00032	ND	ND	ND	51.78
300	1097	530	38.88	0.00054	0.00025	ND	ND	ND	53.26
300	1098	531	37.39	0.00162	0.00024	ND	ND	ND	53.34
300	1098	532	38.20	0.00157	0.00024	ND	ND	ND	53.11
300	1098	534	37.94	0.00146	0.00024	ND	ND	ND	53.55

ND = not detected

Table E.5: Results for other measured species in the products with an oven temperature setpoint of 1073 K and an initial pressure of 399 kPa.

Reaction time (s)	Temperature (K)	Final Pressure (kPa)	Molar Concentration (%)						Scaling Factor*
			CO2	O2	Nitrogen	CO	Helium	Sum	
15	1095	417	0.131	0.619	3.94	ND	ND	97.31	1.0482
15	1093	425	0.248	0.570	3.70	ND	ND	96.09	1.0471
15	1091	424	0.236	0.533	3.57	ND	ND	96.13	1.0452
15	1094	431	0.250	0.508	4.15	ND	ND	96.80	1.0507
15	1089	443	0.286	0.495	3.48	ND	ND	95.08	1.0448
15	1088	442	0.282	0.483	3.42	ND	ND	95.28	1.0439
15	1088	443	0.260	0.504	3.45	ND	ND	95.12	1.0443
30	1093	430	ND	ND	0.93	ND	0.042	99.23	1.0094
30	1090	441	ND	0.032	0.90	ND	0.035	98.69	1.0095
30	1092	432	ND	0.042	1.02	ND	0.034	99.14	1.0108
30	1091	468	0.161	0.541	2.99	ND	ND	95.10	1.0389
30	1092	466	0.202	0.491	3.52	ND	ND	95.03	1.0444

Reaction time (s)	Temperature (K)	Final Pressure (kPa)	Molar Concentration (%)						Scaling Factor*
			CO2	O2	Nitrogen	CO	Helium	Sum	
60	1098	495	0.049	ND	0.46	ND	0.049	97.74	1.0052
60	1096	446	ND	ND	0.63	ND	0.057	99.59	1.0063
60	1095	454	ND	ND	0.76	ND	0.049	99.39	1.0076
60	1094	449	ND	ND	0.79	ND	0.045	99.45	1.0079
60	1095	492	0.162	0.490	3.48	ND	ND	95.14	1.0434
60	1095	490	0.156	0.482	3.41	ND	ND	95.04	1.0426
60	1094	492	0.157	0.475	3.37	ND	ND	95.08	1.0421
180	1095	519	0.113	0.369	2.86	ND	ND	95.15	1.0351
180	1096	518	0.115	0.359	2.82	ND	ND	95.05	1.0347
180	1096	518	0.116	0.365	2.81	ND	ND	94.96	1.0347
180	1096	519	0.118	0.363	2.80	ND	ND	95.02	1.0345
180	1086	520	0.048	ND	0.77	ND	0.032	96.38	1.0085
180	1086	518	ND	ND	0.77	ND	0.025	95.46	1.0080
180	1086	526	0.059	ND	1.02	ND	0.017	96.89	1.0111
180	1090	522	0.051	0.055	1.09	ND	ND	97.26	1.0123
180	1089	527	ND	ND	0.55	ND	0.029	97.36	1.0057
180	1093	525	ND	ND	0.63	ND	0.026	97.50	1.0065
300	1100	521	ND	0.009	0.71	ND	0.027	97.53	1.0074
300	1097	513	ND	0.003	0.82	ND	0.024	97.45	1.0084
300	1101	530	0.110	0.506	3.84	ND	ND	96.42	1.0463
300	1097	530	0.113	0.324	2.54	ND	ND	95.12	1.0313
300	1098	531	0.153	0.592	4.04	ND	ND	95.52	1.0501
300	1098	532	0.148	0.472	3.47	ND	ND	95.40	1.0429
300	1098	534	0.15	0.459	3.36	ND	ND	95.45	1.0416

*Scaling factor is used for normalizing the data.
ND = not detected

Table E.6: Normalized results for hydrocarbons, helium, and hydrogen with oven temperature setpoint at 1073 K and an initial pressure of 399 kPa.

Reaction time (s)	Temperature (K)	Final Pressure (kPa)	Molar Concentration (%)							
			Methane	Ethane	Ethylene	Propane	Acetylene	Benzene	Helium	Hydrogen
15	1095	417	81.58	0.00327	0.00151	ND	ND	0.00063	ND	15.50
15	1093	425	78.27	0.00372	0.00112	ND	ND	ND	ND	17.61
15	1091	424	78.54	0.00386	0.00103	ND	ND	ND	ND	17.39
15	1094	431	75.51	0.00396	0.00073	ND	ND	ND	ND	21.04
15	1089	443	68.16	0.00122	0.00047	ND	ND	ND	ND	26.72
15	1088	442	68.40	0.00176	0.00048	ND	ND	ND	ND	26.69
15	1088	443	67.61	0.00253	0.00046	ND	ND	ND	ND	27.32
30	1093	430	80.94	0.00088	0.00088	ND	ND	ND	0.043	18.23
30	1090	441	74.37	0.00070	0.00062	ND	ND	ND	0.035	24.28
30	1092	432	79.62	0.00111	0.00081	ND	ND	ND	0.034	19.47
30	1091	468	59.32	0.00224	0.00044	ND	ND	ND	ND	35.64
30	1092	466	60.11	0.00083	0.00046	ND	ND	ND	ND	34.74
60	1098	495	55.25	0.00034	0.00042	ND	ND	ND	0.049	42.43
60	1096	446	76.53	0.00056	0.00094	ND	ND	ND	0.057	22.99
60	1095	454	72.64	0.00045	0.00073	ND	ND	ND	0.050	26.70
60	1094	449	74.90	0.00074	0.00083	ND	ND	ND	0.045	24.50
60	1095	492	52.12	0.00209	0.00045	ND	ND	ND	ND	42.84
60	1095	490	52.47	0.00205	0.00046	ND	ND	ND	ND	42.40
60	1094	492	52.47	0.00154	0.00045	ND	ND	ND	ND	42.44
180	1095	519	43.52	0.00159	0.0004	ND	ND	ND	ND	51.50
180	1096	518	44.11	0.00169	0.00042	ND	ND	ND	ND	50.82
180	1096	518	44.03	0.00084	0.00042	ND	ND	ND	ND	50.81
180	1096	519	44.07	0.00163	0.0004	ND	ND	ND	ND	50.83
180	1086	520	47.01	0.00074	0.00046	ND	ND	ND	0.032	49.33
180	1086	518	46.37	ND	0.00042	ND	ND	ND	0.025	49.06
180	1086	526	45.19	0.00086	0.00038	ND	ND	ND	0.018	51.66

Reaction time (s)	Temperature (K)	Final Pressure (kPa)	Molar Concentration (%)							
			Methane	Ethane	Ethylene	Propane	Acetylene	Benzene	Helium	Hydrogen
180	1090	522	45.98	0.00085	0.00041	ND	ND	ND	ND	51.26
180	1089	527	45.49	0.00092	0.00041	ND	ND	ND	0.029	51.84
180	1093	525	46.26	ND	0.00045	ND	ND	ND	0.026	51.21
300	1100	521	49.43	0.00071	0.00082	ND	ND	ND	0.027	48.06
300	1097	513	50.94	0.00220	0.00093	ND	ND	ND	0.024	46.48
300	1101	530	42.04	0.00255	0.00033	ND	ND	ND	ND	54.18
300	1097	530	40.10	0.00056	0.00025	ND	ND	ND	ND	54.93
300	1098	531	39.26	0.00170	0.00026	ND	ND	ND	ND	56.02
300	1098	532	39.83	0.00164	0.00025	ND	ND	ND	ND	55.39
300	1098	534	39.51	0.00152	0.00025	ND	ND	ND	ND	55.77

ND = not detected

Table E.7: Results for hydrocarbons and hydrogen with an oven temperature setpoint of 1273 K and an initial pressure of 399 kPa.

Reaction time (s)	Temperature (K)	Final Pressure (kPa)	Molar Concentration (%)						
			Methane	Ethane	Ethylene	Propane	Acetylene	Benzene	Hydrogen
15	1294	459	63.23	0.0509	0.367	ND	0.04298	0.142735	29.07
15	1293	460	61.42	0.0470	0.401	ND	0.04797	0.145386	30.97
15	1291	460	61.32	0.0450	0.393	ND	0.04829	0.142812	30.47
30	1293	472	59.58	0.0375	0.277	ND	0.03695	0.101494	33.77
30	1293	469	58.84	0.0376	0.272	ND	0.03450	0.093558	33.12
30	1289	461	58.77	0.0262	0.239	ND	0.01497	0.041928	33.29
60	1296	485	53.47	0.0247	0.148	ND	0.01508	0.029889	38.10
60	1296	482	52.99	0.0214	0.139	ND	0.01391	0.030496	38.72
60	1297	485	55.91	0.0295	0.186	ND	0.02067	0.037555	37.26
60	1296	485	56.51	0.0336	0.220	ND	0.02189	0.053617	36.81
60	1289	478	52.68	0.0151	0.085	ND	0.00178	0.000960	38.90
180	1287	529	44.80	0.0062	0.020	ND	ND	ND	51.02

Reaction time (s)	Temperature (K)	Final Pressure (kPa)	Molar Concentration (%)						
			Methane	Ethane	Ethylene	Propane	Acetylene	Benzene	Hydrogen
180	1284	530	43.06	0.0059	0.020	ND	0.00019	ND	51.36
180	1284	522	43.51	0.0056	0.021	ND	0.00020	ND	50.85
180	1283	530	44.13	0.0056	0.016	ND	0.00019	ND	52.27
180	1286	532	43.05	0.0055	0.016	ND	0.00021	ND	52.92
180	1285	536	42.38	0.0050	0.014	ND	0.00019	ND	53.34
300	1296	509	53.09	0.0272	0.168	ND	0.00782	0.017051	44.51
300	1296	518	51.58	0.0233	0.123	ND	0.00407	0.010255	45.14
300	1296	533	46.17	0.0141	0.040	ND	0.00147	0.000907	49.90
300	1296	533	45.68	0.0117	0.037	ND	0.00166	0.000096	50.01
300	1294	542	36.67	0.0070	0.011	ND	0.00037	0.003440	55.88
300	1298	533	37.05	0.0053	0.011	ND	0.00024	0.000106	53.61
300	1297	533	42.30	0.0104	0.026	ND	0.00069	0.000080	51.21
300	1295	533	43.82	0.0135	0.042	ND	0.00124	0.004845	50.02
300	1296	535	42.43	0.0111	0.026	ND	0.00065	0.000181	51.50
300	1294	556	38.20	0.0115	0.036	ND	ND	0.007296	56.72
300	1287	560	38.86	0.0040	0.006	ND	ND	0.000000	57.98
300	1292	544	40.80	0.0133	0.038	ND	ND	0.006864	53.29

ND = not detected

Table E.8: Results for other measured species in the products with an oven temperature setpoint of 1273 K and an initial pressure of 399 kPa.

Reaction time (s)	Temperature (K)	Final Pressure (kPa)	Molar Concentration (%)						Scaling Factor*
			CO2	O2	Nitrogen	CO	Helium	Sum	
15	1294	459	ND	0.624	3.59	ND	ND	97.11	1.0434
15	1293	460	ND	0.578	3.44	ND	ND	97.05	1.0414
15	1291	460	ND	0.706	3.79	ND	ND	96.91	1.0464
30	1293	472	ND	0.531	3.28	ND	ND	97.61	1.0390
30	1293	469	ND	0.627	3.82	ND	ND	96.85	1.0460

Reaction time (s)	Temperature (K)	Final Pressure (kPa)	Molar Concentration (%)						Scaling Factor*
			CO2	O2	Nitrogen	CO	Helium	Sum	
30	1289	461	0.046	0.509	3.24	ND	ND	96.17	1.0395
60	1296	485	ND	0.652	3.88	ND	ND	96.32	1.0471
60	1296	482	ND	0.486	3.10	ND	ND	95.51	1.0376
60	1297	485	ND	0.480	3.06	ND	ND	96.98	1.0365
60	1296	485	ND	0.474	3.06	ND	ND	97.19	1.0364
60	1289	478	0.058	0.552	3.28	ND	ND	95.57	1.0407
180	1287	529	ND	ND	0.56	ND	0.038	96.44	1.0058
180	1284	530	ND	ND	0.81	ND	0.027	95.29	1.0085
180	1284	522	ND	0.051	1.05	ND	0.016	95.50	1.0115
180	1283	530	ND	ND	0.29	ND	0.038	96.76	1.0030
180	1286	532	ND	ND	0.46	ND	0.032	96.48	1.0048
180	1285	536	ND	ND	0.69	ND	0.021	96.45	1.0072
300	1296	509	ND	0.067	0.91	ND	0.034	98.84	1.0099
300	1296	518	ND	0.099	1.11	ND	0.023	98.11	1.0123
300	1296	533	ND	0.096	1.10	ND	0.016	97.34	1.0123
300	1296	533	ND	0.112	1.18	ND	ND	97.03	1.0133
300	1294	542	ND	0.380	2.57	ND	ND	95.52	1.0309
300	1298	533	0.050	0.626	3.98	ND	ND	95.34	1.0488
300	1297	533	ND	0.488	3.20	ND	ND	97.23	1.0380
300	1295	533	ND	0.469	3.10	ND	ND	97.47	1.0366
300	1296	535	ND	0.455	2.99	ND	ND	97.41	1.0354
300	1294	556	ND	0.306	2.43	ND	ND	97.72	1.0280
300	1287	560	ND	0.076	0.93	ND	ND	97.86	1.0103
300	1292	544	ND	0.429	3.14	ND	ND	97.71	1.04

*Scaling factor is used for normalizing the data.
ND = not detected

Table E.9: Normalized results for hydrocarbons, helium, and hydrogen with oven temperature setpoint at 1273 K and an initial pressure of 399 kPa.

Reaction time (s)	Temperature (K)	Final Pressure (kPa)	Molar Concentration (%)							
			Methane	Ethane	Ethylene	Propane	Acetylene	Benzene	Helium	Hydrogen
15	1294	459	65.97	0.0531	0.383	ND	0.04484	0.148927	ND	30.33
15	1293	460	63.96	0.0490	0.418	ND	0.04996	0.151408	ND	32.25
15	1291	460	64.16	0.0471	0.411	ND	0.05053	0.149436	ND	31.88
30	1293	472	61.90	0.0390	0.287	ND	0.03839	0.105456	ND	35.09
30	1293	469	61.54	0.0394	0.285	ND	0.03608	0.097857	ND	34.65
30	1289	461	61.09	0.0272	0.249	ND	0.01557	0.043584	ND	34.60
60	1296	485	55.98	0.0258	0.155	ND	0.01579	0.031296	ND	39.90
60	1296	482	54.99	0.0222	0.144	ND	0.01444	0.031643	ND	40.17
60	1297	485	57.95	0.0305	0.192	ND	0.02143	0.038927	ND	38.62
60	1296	485	58.57	0.0349	0.228	ND	0.02268	0.055568	ND	38.15
60	1289	478	54.83	0.0157	0.088	ND	0.00185	0.001000	ND	40.48
180	1287	529	45.06	0.0063	0.020	ND	ND	ND	0.038	51.31
180	1284	530	43.43	0.0060	0.020	ND	0.00019	ND	0.027	51.80
180	1284	522	44.01	0.0057	0.021	ND	0.00020	ND	0.016	51.43
180	1283	530	44.27	0.0056	0.017	ND	0.00019	ND	0.038	52.43
180	1286	532	43.25	0.0056	0.017	ND	0.00021	ND	0.032	53.17
180	1285	536	42.69	0.0050	0.014	ND	0.00019	ND	0.021	53.72
300	1296	509	53.62	0.0274	0.169	ND	0.00790	0.017220	0.035	44.95
300	1296	518	52.21	0.0236	0.125	ND	0.00412	0.010381	0.023	45.69
300	1296	533	46.74	0.0143	0.041	ND	0.00149	0.000919	0.016	50.51
300	1296	533	46.29	0.0119	0.038	ND	0.00168	0.000097	ND	50.68
300	1294	542	37.80	0.0072	0.012	ND	0.00038	0.003546	ND	57.60
300	1298	533	38.86	0.0055	0.012	ND	0.00025	0.000111	ND	56.23
300	1297	533	43.90	0.0108	0.027	ND	0.00071	0.000083	ND	53.15
300	1295	533	45.43	0.0140	0.044	ND	0.00129	0.005022	ND	51.85

Reaction time (s)	Temperature (K)	Final Pressure (kPa)	Molar Concentration (%)							
			Methane	Ethane	Ethylene	Propane	Acetylene	Benzene	Helium	Hydrogen
300	1296	535	43.93	0.0115	0.026	ND	0.00067	0.000187	ND	53.32
300	1294	556	39.28	0.0118	0.037	ND	ND	0.007500	ND	58.31
300	1287	560	39.26	0.0040	0.006	ND	ND	ND	ND	58.58
300	1292	544	42.28	0.0138	0.039	ND	ND	0.007115	ND	55.23

ND = not detected

Table E.10: Average final pressure and its uncertainty for all reaction times at different temperatures

	Temperature (K)		
	892	1093	1292
Reaction time (s)	Final Pressure (kPa)	Final Pressure (kPa)	Final Pressure (kPa)
15	424.8 ± 12.2	432.2 ± 8.6	459.8 ± 3.6
30	443.3 ± 7.7	447.4 ± 17.9	467.3 ± 10.8
60	451.6 ± 7.6	473.8 ± 17.2	482.9 ± 3.7
180	465.3 ± 3.9	521.4 ± 4.0	529.6 ± 5.1
300	469.0 ± 2.2	527.1 ± 6.4	535.7 ± 8.1